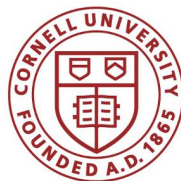

Zodi Project Final MEng Report:
Design of a 4U CubeSat for
Face-On Imaging of the Zodiacal Dust Cloud
from Outside the Ecliptic Plane

Dante Del Terzo

Sibley School of Mechanical and Aerospace Engineering
Cornell University
Ithaca, New York, USA

Supervisor:
Professor Dmitry Savransky

May 23, 2018



Project Team Members:

Faculty Supervisor:

Dmitry Savransky (*ds264@cornell.edu*)

MEng Project Lead (Fall 2017 - Spring 2018):

Dante Del Terzo (*dnd37@cornell.edu*)

Spring 2018 Undergraduate Team Members:

Aaron Brown (*ahb68@cornell.edu*)

Chris Della Santina (*cld228@cornell.edu*)

Xinwei Liu (*xl359@cornell.edu*)

Fall 2017 Undergraduate Team Members:

Amlan Sinha (*as2558@cornell.edu*)

Chris Della Santina (*cld228@cornell.edu*)

Niharika Shukla (*ns596@cornell.edu*)

Xinwei Liu (*xl359@cornell.edu*)

Flight Trajectory Analysis:

Gabriel Soto (*gs635@cornell.edu*)

Contents

Abstract	4
1 Introduction	5
2 Mission Overview	6
2.1 Mission Requirements	6
2.2 Mission Storyboard	6
3 Extracting Orbital Parameters	9
3.1 Early Calculations	9
3.2 Extracting Exact Parameters from ZODIStatesAfterInitialFlyby.mat	10
4 Subsystem Analysis	12
4.1 Scientific Optical Payload (Camera)	12
4.1.1 Analysis	12
4.1.2 Recommendations for Future Work	14
4.2 Propulsion Subsystem	14
4.2.1 Analysis	14
4.2.2 Recommendations for Future Work	16
4.3 Communications Subsystem	17
4.3.1 Analysis	17
4.3.2 Recommendations for Future Work	18
4.4 Command & Data Handling Subsystem	18
4.4.1 Analysis	19
4.4.2 Recommendations for Future Work	19
4.5 Power Subsystem	19
4.5.1 Solar Array Analysis	20
4.5.2 Battery Sizing Analysis	22
4.5.3 Recommendations for Future Work	23
4.6 Attitude Control & Determination Subsystem	24
4.6.1 Attitude Determination Analysis	24
4.6.2 Attitude Control Analysis	24
4.6.3 Recommendations for Future Work	26
4.7 Thermal Analysis	26
4.7.1 Analysis	26
4.7.2 Recommendations for Future Work	29
4.8 Structure	30
4.8.1 Analysis	30
4.8.2 Recommendations for Future Work	30
5 Conclusions	31
6 Acknowledgements	31
Appendices	32
A Mass & Volume Budget	32
B Power Budget	33
C Link Budget	34
D MATLAB Code	37
D.1 ZODItrajectory.m	37
D.2 ZODIpanelDegradation.m	47
D.3 ZODIphototime.m	50
References	51

Abstract

In this report we explore the feasibility of using a 4U CubeSat to image the zodiacal dust cloud from a face-on perspective above the ecliptic plane. To do this, trade studies and analyses of various subsystem components were performed to ensure each subsystem could meet the requirements of this mission. Within two semesters we were able to complete this feasibility analysis for all subsystems and determine that this ZODI mission could be accomplished with a 4U CubeSat.

1 Introduction

The ZODI CubeSat Project Team’s goal is to design, build, and launch a CubeSat tasked with detaching from a larger payload, getting at least 0.10AU above the elliptic disk, taking face-on photographs of the Zodiacal Dust Cloud, then transmitting that data back to Earth. Over the course of the Fall 2017 and Spring 2018 terms, analysis was performed in order to assess the feasibility of accomplishing this task with a CubeSat less than 6U in size.

Our current flight trajectory was simulated and put forth by Gabriel Soto in his paper “*Optimization of high-inclination orbits using planetary flybys for a zodiacal light-imaging mission*” [1], in which he proposes using the EVE transfer maneuver originally proposed for the 2022 Europa Clipper mission as a jumping-off point for a zodiacal light imaging CubeSat mission. Following his analysis, deploying from the Europa Clipper after the Venus flyby of its EVE maneuver, 68% of the way to the next flyby of Earth, a single Δv burn of 37.21m/s in conjunction with the resulting Earth gravity assist would produce an elliptic orbit with apoapsis 0.22 AU above the solar elliptic disk and periapsis 0.13AU below the solar elliptic disk. This orbit will have an orbital period of one Earth year (365.1653 day orbital period), ensuring it will intercept the Earth a year later with a closest approach of 8371km.

A potentially different trajectory utilizing solar sails was researched by Amlan Sinha in the Fall 2017 semester, but was ultimately not selected. The infancy of solar sail technology as well as difficulties getting the CubeSat back into Earth transmission range ultimately resulted in the decision to choose the previously mentioned EVE method to achieve our desired orbital height.

Through this year-long analysis, we have concluded that a 4U CubeSat will be sufficient to complete this mission. Below in Figure 1, a CAD model of our Zodi CubeSat design while fully deployed is shown. Figure 2 shows a preliminary arrangement of the Zodi CubeSat interior.

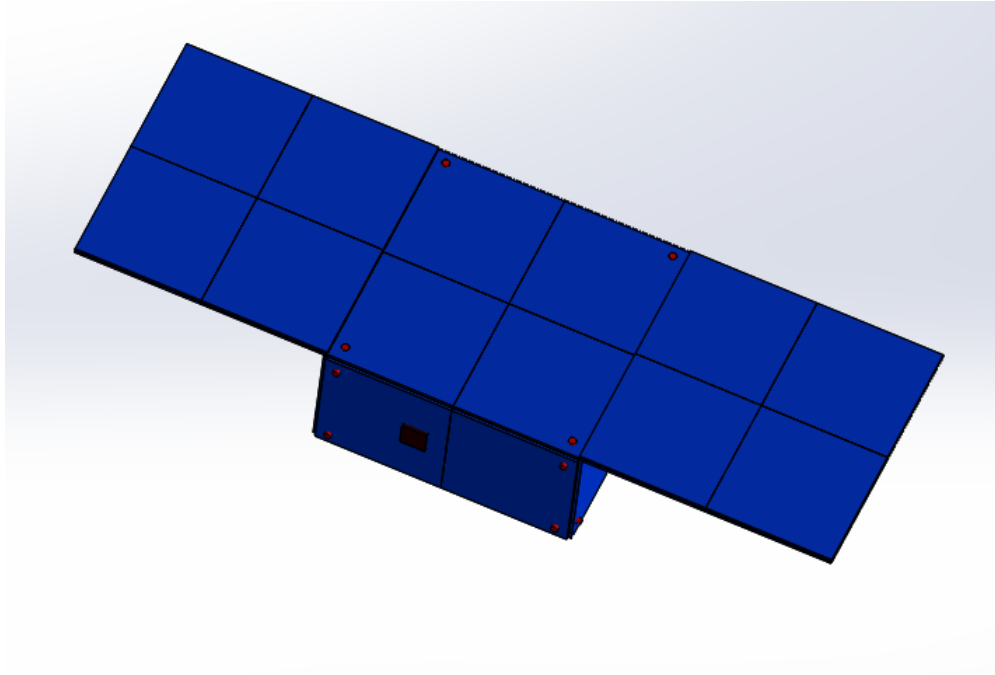


Figure 1: CAD model of our Zodi CubeSat fully deployed. See Figure 2 for internal view.

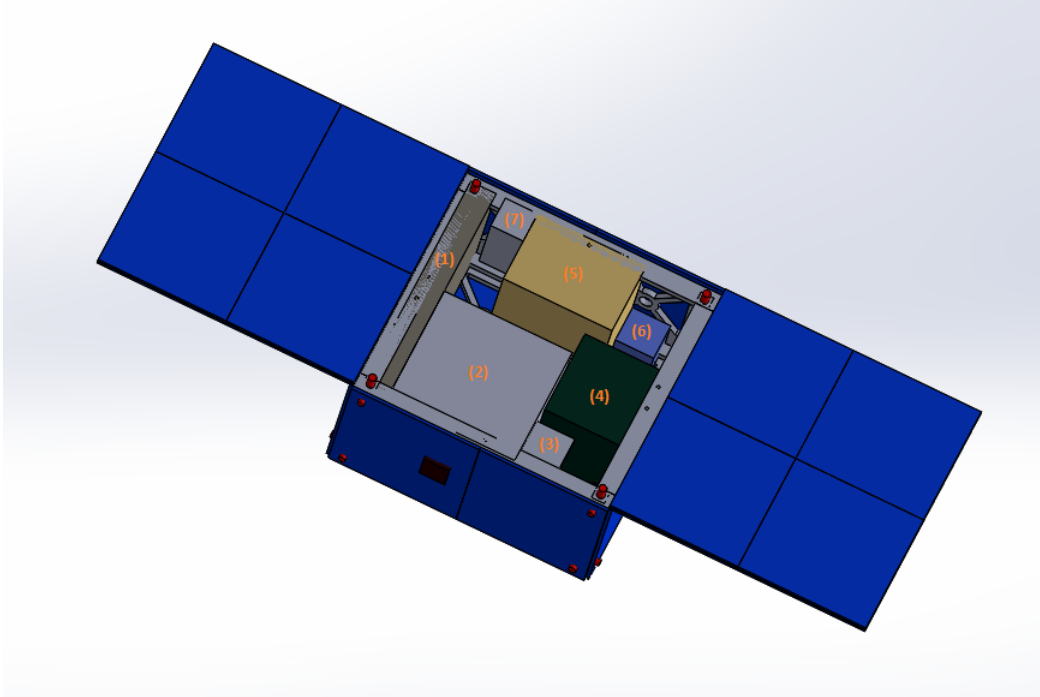


Figure 2: Internal view of our fully deployed Zodi CubeSat CAD model. (1) Li-Ion Battery. (2) Camera (Outward facing lens visible below on exterior). (3) Transmitter. (4) Reaction Wheel Assembly. (5) BET Electropray Thruster. (6) Electropray Thruster Fuel Tank. (7) Cold-Gas Momentum Dumping System Fuel Tank. Momentum dumping thrusters represented as red pegs.

2 Mission Overview

2.1 Mission Requirements

Table 1: System-Level Requirements for the Zodi CubeSat Mission

Requirement ID	System-Level Requirements
REQ 1	The CubeSat must be below 6U in volume
REQ 2	The CubeSat must be able to accomplish all mission goals autonomously after deployment
REQ 3	The CubeSat must reach a height of at least 0.1AU above the ecliptic in order to properly image the zodiacal cloud
REQ 4	The CubeSat must be able to capture at least one full horizon of images
REQ 5	The CubeSat must be able to operate for a 1 Earth year lifecycle after deployment until data collection and transmission is completed
REQ 6	The CubeSat must be able to store all collected data onboard until transmission approximately 1 Earth year after deployment
REQ 7	The CubeSat must be able to transmit all collected data back to Earth

2.2 Mission Storyboard

Event 1: Launch & Transit (Undeployed)

The Zodi CubeSat will be housed in a 4U CubeSat deployment pod attached to the body of the Europa Clipper inside the launch vehicle fairing. Both the CubeSat and deployment pod will be designed to handle the gravitational, thermal, and vibrational loads associated with the specific launch vehicle. After exiting Earth's atmosphere, the CubeSat will remain attached to

the Europa clipper during the (first) Earth and Venus sections of its EVE gravitational assist maneuver until CubeSat deployment occurs at Event 2.

Event 2: CubeSat Deployment & Initialization

After the Europa Clipper performs its Venusian gravitational assist, the Zodi CubeSat will jettison from its deployment pod and begin startup initialization. During this time it will initialize its electronic systems and deploy its deployable solar array and antenna. The resulting initialization and gyroscopic data will be transmitted for several hours using its omnidirectional X-Band antenna (Communications Subsystem detailed in Section 4.3). If possible, the Deep Space Network (DSN) will be used to monitor for and receive this transmission, allowing the ground crew to confirm whether or not deployment and/or electronic initialization was successful. If either were unsuccessful, the ground crew will have until the inclination change burn in Event 3 Zodi CubeSat (when the CubeSat has traveled 68% of the way back to Earth) to diagnose the problem and upload a software fix using the DSN.

In the case where DSN monitoring time cannot be acquired, it will be entirely up to the Zodi CubeSat's autonomous programming (Command & Data Handling Subsystem detailed in Section 4.4) to determine whether deployment and initialization has occurred successfully and attempt to fix the problem if it has not. The autonomous system will be designed to attempt to fix the most probable deployment and startup errors even in the case where DSN monitoring time CAN be acquired.

After a successful startup and/or fixing any errors in deployment and initialization. The CubeSat will proceed along its trajectory until it has traveled 68% of the way to Earth, at which time it will begin its inclination change burn in Event 3. While in transit, the CubeSat will charge its backup Li-Ion battery.

Event 3: Inclination Change & Earth Gravity Assist

68% of the way to Earth, the CubeSat will fire its electro-spray thruster (Propulsion Subsystem detailed in Section 4.2) and execute a single Δv burn of 37.21m/s. The CubeSat will accomplish this burn using either the BET-1mN or BET-100 μ N electro-spray thruster, completing the burn in 3.2 or 18.9 days, respectively. This burn, along with the final Earth gravity assist will increase the inclination of the Zodi CubeSat's orbit by an orbital height of 0.1283AU at periapsis, resulting in a final heliocentric orbit with periapsis located 0.1283AU below the ecliptic, apoapsis located 0.2215AU above the ecliptic, and an orbital period of approximately one Earth year. This orbital period will ensure that the CubeSat will re-intercept Earth one year later to transmit its scientific data. For a brief moment, the sun may be eclipsed by the Earth during this gravity assist. If an eclipse should occur, power will be provided by the CubeSat's Li-Ion battery (Li-Ion Battery detailed in Section 4.5.2)

This final Earth gravitational assist also represents the first and last time that the ground crew will be able to contact the CubeSat without the need of the DSN until it returns to transmit its scientific data one year later. If DSN monitoring time could not be acquired in Event 2, the ground crew will have one last chance to receive startup data, diagnose any issues, and upload a software patch.

After completing its insertion into its final mission orbit, the CubeSat will begin transit to periapsis. It will take approximately 68.4208 days to reach periapsis. While in transit, the

CubeSat will enter a standby mode and recharge its backup Li-Ion battery to capacity.

Event 4: Image Collection at Periapsis

Upon reaching periapsis, the Zodi CubeSat will begin face-on imaging of the Zodiacal Dust Cloud. This event represents the point at which the CubeSat will reach its highest temperature (Thermal Analysis detailed in Section 4.7). The solar array has been sized to provide sufficient power to the CubeSat subsystems during this imaging process without the need for a battery, though the Li-Ion battery will be able to provide additional power if necessary (Power Subsystem detailed in Section 4.5).

Upon nearing periapsis, the CubeSat will use its ACDS system to determine the direction of the Zodi Cloud and orient itself accordingly (ACDS Subsystem detailed in Section 4.6). To ensure the entire Zodi Cloud is imaged, the CubeSat's optical payload (Optical Payload detailed in Section 4.1) will capture the full horizon in 232 images. This imaging process will take 9.67 days. After each image is captured, it will be stored in the CubeSat's on-board harddrive and redundantly copied to protect the data from cosmic radiation bit flips (See Section 4.4).

After capturing and storing a full horizon of images, the Zodi CubeSat will reenter standby mode and recharge its Li-Ion battery if necessary. It will take approximately 172.9325 days for the CubeSat to reach the next event at apoapsis.

Event 5: Image Collection at Apoapsis

Upon reaching apoapsis, the Zodi CubeSat will once again begin face-on imaging of the Zodiacal Dust Cloud. This event represents the point at which the CubeSat will reach its lowest temperature (See Section 4.7). The solar array has been sized to provide sufficient power to the CubeSat subsystems without the need for a battery even at apoapsis, though the Li-Ion battery will be able to provide additional power if necessary (See Section 4.5).

Upon nearing apoapsis, the CubeSat will once again use its ACDS system to determine the direction of the Zodi Cloud and orient itself accordingly (See Section 4.6). To ensure the entire Zodi Cloud is imaged, the CubeSat's optical payload (See Section 4.1) will once again capture the full horizon in 232 images. This imaging process will take 9.67 days. Like at periapsis, each image will be stored in the CubeSat's on-board harddrive and redundantly copied to protect the data from cosmic radiation bit flips (See Section 4.4).

After capturing and storing another full horizon of images, the Zodi CubeSat will once again reenter standby mode and recharge its Li-Ion battery if necessary. It will take approximately 104.2983 days for the CubeSat to reach its altitude of closest approach with Earth, where it can begin transmission of its collected image data.

Event 6: Data Transmission on Earth Flyby

After collecting its final horizon of Zodi Cloud images at apoapsis, the CubeSat will re-intercept Earth's orbit approximately one year after inserting into its final orbit. The CubeSat will pass Earth at an altitude of closest approach of 8371 km (See Listing 1). This distance represents the best time for our CubeSat to transmit its data. Using either the Near-Earth Network (NEN) or DSN (See Link Budget in Appendix C), the CubeSat will transmit all of its collected data using an X-Band Transmitter and omni-directional antenna (See Section 4.3). If

transmitting to the DSN, this transmission will take 68 seconds. If transmitting to the NEN, this transmission will take 1.93 hours.

After transmitting all of its data, the primary mission of the Zodi CubeSat will be over. After this point, additional software could be uploaded to the CubeSat to have it pursue additional imaging missions suitable to its high inclination and hardware. Alternatively, the CubeSat could be left to autonomously collect and transmit additional image data until its systems fail. In either case, the completion of this event marks the successful completion of the Zodi CubeSat zodiacal light imaging mission.

3 Extracting Orbital Parameters

3.1 Early Calculations

As stated previously, the working trajectory for our Zodi CubeSat is based on calculations laid out by Gabriel Soto in his paper [1]. However, prior to the receiving the ZODIstatesAfter-FinalFlyby.mat file from Gabriel Soto, rough calculations were performed to determine the CubeSat's approximate final orbital parameters for initial sizing estimates. These approximate orbital parameters were determined using only the orbital height above the ecliptic at apoapsis, the orbital height below the ecliptic at periapsis, and the trajectory plot given in Gabriel Soto's paper [1].

Based on the knowledge that the CubeSat's final orbit has an orbital period ratio with respect to earth of 1, the orbital period of the CubeSat was determined to be approximately 365 days (or $3.154e7$ seconds). From this orbital period, the approximate mean motion, n , and approximate semi-major axis, a , were calculated:

$$n \approx \frac{2\pi}{P_{Earth}} = \frac{2\pi}{1 \text{ year}} = \frac{2\pi}{3.154e7 \text{ sec}} = 1.992e-7 \text{ rad/s}$$

$$a \approx \sqrt[3]{\frac{\mu_{sun}}{n^2}} = \sqrt[3]{\frac{1.32712440041e20 \text{ m}^3/\text{s}^2}{(1.992e-7 \text{ rad/s})^2}} = 1.4954e11 \text{ m}$$

Looking at Figure 8 in Gabriel Soto's paper [1], it was determined that the X and Y values of the CubeSat's periapsis are approximately equal to the X and Y values of Venus' orbital radius, $\approx 1.082e11$ m from the Sun. According to Gabriel Soto's calculations, shown in the rightmost column of Table 2 of Gabriel Soto's paper [1], the periapsis of the CubeSat's orbit is approximately 0.1283 AU ($1.9193e10$ m) below the ecliptic. Using these values and Pythagoras' theorem, approximate values for the orbital radius at periapsis, r_p , and inclination, i , of our CubeSat were calculated:

$$r_p \approx \sqrt{(r_{venus})^2 + (z_{peri})^2} = \sqrt{(1.082e11 \text{ m})^2 + (1.9193e10 \text{ m})^2} = 1.09889e11 \text{ m}$$

$$i \approx \arctan \frac{z_{peri}}{r_{venus}} = \arctan \frac{1.9193e10 \text{ m}}{1.082e11 \text{ m}} = 10.05875^\circ$$

With these values, approximate values for the eccentricity, e , the radius at apoapsis, r_a , the semi-parameter, p , the velocity at periapsis, v_p , and the velocity at apoapsis, v_a , were

calculated:

$$e \approx 1 - \frac{r_p}{a} = 1 - \frac{1.09889e11 \text{ m}}{1.4954e11 \text{ m}} = 1 - 0.2651 = 0.26515$$

$$r_a \approx a(1 + e) = (1.4954e11 \text{ m})(1 + 0.26515) = 1.8919e11 \text{ m}$$

$$p \approx a(1 - e^2) = (1.4954e11 \text{ m})(1 - 0.26515^2) = 1.39e11 \text{ m}$$

$$v_p \approx \sqrt{\frac{\mu_{sun}}{r_p}(1 - e)} = \sqrt{\frac{1.32712440041e20 \text{ m}^3/\text{s}^2}{1.09889e11 \text{ m}}(1 - 0.26515)} = 39088.564 \text{ m/s}$$

$$v_a \approx \sqrt{\frac{\mu_{sun}}{r_p}(1 + e)} = \sqrt{\frac{1.32712440041e20 \text{ m}^3/\text{s}^2}{1.09889e11 \text{ m}}(1 + 0.26515)} = 22704.19341 \text{ m/s}$$

These values provided us with working orbital parameter data until more exact parameters could be extracted from the .mat file provided by Gabriel Soto. It is worth noting that the maximum percent error between any rough calculation and its more exact .mat counterpart was only 2.93%. After obtaining the .mat file from Gabriel Soto, the full orbital data was extracted and these approximate values were no longer necessary. All data and calculations presented in this paper, where applicable, use the more exact orbital parameter values extracted from ZODIstatesAfterFinalFlyby.mat as described in Section 3.2.

3.2 Extracting Exact Parameters from ZODIstatesAfterInitialFlyby.mat

The ZODIstatesAfterFinalFlyby.mat MATLAB file contains the X, Y, and Z coordinates of the CubeSat's position and velocity vectors relative to the sun for its proposed final orbit, propagated across 30000 timesteps. ZODIstatesAfterFinalFlyby.mat simulates the orbit of our CubeSat for 3 complete orbits across 800.216 days with 30000 timesteps of 2304.699 seconds (38.4117 minutes) each. The orbital trajectory of the CubeSat after its inclination change but prior to its first Earth transmission window is shown below in Figure 3 (3D View) and Figure 4 (Top-Down View):

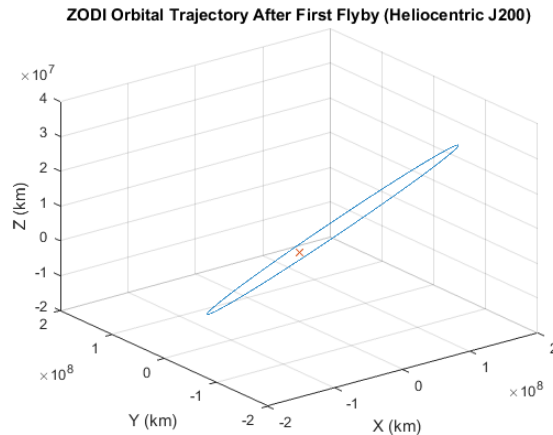


Figure 3: A 3D plot of the orbital trajectory of the Zodi CubeSat after completing its inclination change but before the first Earth transmission window. The position of the sun is shown as a red 'X'.

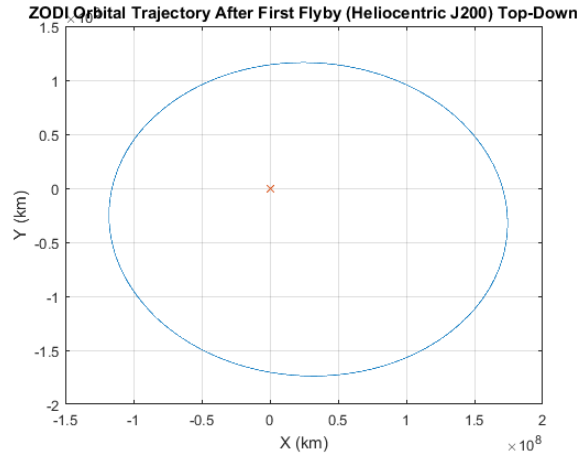


Figure 4: A top-down plot of the orbital trajectory of the Zodi CubeSat after completing its inclination change but before the first Earth transmission window. The position of the sun is shown as a red 'X'.

In addition to determining the time of simulation and plotting the trajectory, ZODItrajectory.m also extracts more precise orbital parameters for this simulated final orbit. The orbital elements and more are contained in the printed output from the "Trajectory & Orbit Info" section of the ZODItrajectory.m script, shown below in Listing 1. All calculations presented in this paper, where appropriate, use the orbital elements listed below in Listing 1:

```

R_periapsis: 108748530.4715 km
V_periapsis: 39.4138 km/s
PeriIndex: 2748
5 R_apoapsis: 190397164.4198 km
V_apoapsis: 22.5118 km/s
ApoIndex: 9595

Orbital Elements:
10 a = 149572847.4456 km
p = 138430284.575 km
e = 0.27294
i = 9.7723 deg
n = 1.9915e-07 rad/s
15 Period = 365.1653 days

Total Time of Simulation = 800.216 days
Time Between Datapoints = 2304.699 sec = 38.4117 min
Time Between Orbit Insertion & Peri Data Collect = 5911553.0535 sec = 1642.0981 hours =
  ↳ 68.4208 days
20 Time Between Peri Data & Apo Data Collect = 14941363.9166 sec = 4150.3789 hours = 172.9325
  ↳ days
Time Between Apo Data Collect & Earth Transmit = 9011373.2707 sec = 2503.1592 hours =
  ↳ 104.2983 days
Index of Earth Transmit: 13690

Time Req To Transmit Data to Earth (DSN): 68 sec = 0.018889 hours
25 Time Req To Transmit Data to Earth (NEN): 6931.1724 sec = 1.9253 hours

```

Listing 1: Output of the "Trajectory & Orbit Info" section of the ZODItrajectory.m MATLAB script. See full ZODItrajectory.m script in Appendix D.1

4 Subsystem Analysis

4.1 Scientific Optical Payload (Camera)

Table 2: Scientific Optical Payload (Camera) Requirements for the Zodi CubeSat Mission

Requirement ID	Scientific Optical Payload (Camera) Subsystem Requirements	Mapping to System-Level Requirements
CAM-REQ 1	The resolution of the optical payload must be high enough to properly resolve the shape of the Zodiacal Cloud.	REQ 4
CAM-REQ 2	The optical payload must be able to image a full horizon of Zodiacal Cloud images at both periapsis and apoapsis.	REQ 4
CAM-REQ 3	The size of the optical payload must be small enough to ensure that it does not put the total size of the CubeSat above 6U.	REQ 1

4.1.1 Analysis

Table 3: Parameters of multiple image sensors analyzed for use on the Zodi CubeSat. The selected image sensor, the ADCS-2120 Monochrome sensor, is highlighted.

Image Sensor:	UI-1462LE	uCAM-III	MT9M001	OV7648	ADCS-2120 Monochrome	AM41V4	OV7620
Resolution (h-pixel x v-pixel)	2048 x 1536 pix	640 x 480 pix	1280 x 1024 pix	640 x 480 pix	640 x 480 pix	2336 x 1728 pix	664 x 492 pix
Horiz. Resolution (pixel)	2048 pix	640 pix	1280 pix	640 pix	640 pix	2336 pix	664 pix
Max Resolution (total pixels)	3145728 pix	307200 pix	1310720 pix	307200 pix	307200 pix	4036608 pix	326688 pix
Max Resolution (meter/pixel)	273723.37 m/pix	481125 m/pix	445040.625 m/pix	481125 m/pix	649518.75 m/pix	633444.6347 m/pix	626042.1687 m/pix
Optical Sensor Type	1/2" CMOS	1/4" CMOS	1/2" CMOS	1/4" CMOS	1/3" CMOS	4/3" CMOS	1/3" CMOS
Pixel Size ($\mu\text{m} \times \mu\text{m}$)	3.2 μm	5.55 μm	5.2 μm	5.6 μm	7.4 μm	7 μm	7.6 μm
Optical Sensor Width (mm)	6.554 mm	3.6 mm	6.66 mm	3.6 mm	4.86 mm	17.3 mm	4.86 mm
Assumed Focal Length (mm)	225 mm	225 mm	225 mm				
Horizontal Angular FoV (rad)	0.0291268 rad	0.0159997 rad	0.0295978 rad	0.0159997 rad	0.0215992 rad	0.0768510 rad	0.0215992 rad
Horizontal FoV at Periapsis (m)	560585466.7 m	307920000 m	569652000 m	307920000 m	415692000 m	1479726667 m	415692000 m
Horizontal FoV at Apoapsis (m)	967807333.3 m	531600000 m	983460000 m	531600000 m	717660000 m	2554633333 m	717660000 m
Min. # of pictures per full horizon	172	313	169	313	232	65	232
Frames Per Second (for reference)	11.2 fps	N/A	30 fps	30 fps	25.8 fps	500 fps	25 fps
Max Color Bit Depth (bit)	8 bit	16 bit	10 bit	8 bit	10 bit	10 bit	16 bit
Min. Megabits per full horizon (Mb)	4131 Mb	1469 Mb	2117 Mb	734 Mb	680 Mb	2511 Mb	1157 Mb
Max Operating Power (W)	0.7 W	0.45 W	0.363 W	0.04 W	0.2 W	1.7 W	0.12 W
Standby Power (W)	0.4 W	0.375 W	0.000295 W	0.00003 W	0.0033 W	N/A	0.00001 W
Max Operating Temp (Tested) ($^{\circ}\text{C}$)	55 $^{\circ}\text{C}$	85 $^{\circ}\text{C}$	70 $^{\circ}\text{C}$	70 $^{\circ}\text{C}$	65 $^{\circ}\text{C}$	N/A	N/A
Datasheet	[6]	[7]	[8]	[9]	[2]	[10]	[11]

The Zodi CubeSat’s camera is comprised of an ADCS-2120 monochrome image sensor [2] at the center of a 1U Cassegrain optical telescope setup, modeled after the STARE pathfinder’s optical payload [3]. The CubeSat’s camera represents the scientific payload for this zodiacal light imaging mission. Because of the importance of this subsystem, a trade study was performed comparing numerous image sensors. The parameters of the most promising image sensors that were analyzed are shown above in Table 3. Using these parameters a Pugh matrix was assembled, shown below in Table 4, and from this the ADCS-2120 Monochrome image sensor was selected.

Table 4: Pugh matrix comparing the multiple image sensors analyzed for use on the Zodi CubeSat. The UI-1462LE-C is used as the reference for this Pugh matrix. Using this Pugh matrix, the ADCS-2120 Monochrome image sensor was selected (highlighted in table).

Image Sensor:	UI-1462LE (Reference)	uCAM-III	MT9M001	OV7648	ADCS-2120 Monochrome	AM41V4	OV7620
Max Resolution (Every 50000m/pix diff. is +/-)	0	+++	+++	+++	++++++	++++++	++++++
Min. # of pictures per full horizon (Every 50 pic diff. is +/-)	0	--	EQ	--	+	++	-
Max Color Bit Depth	0	++	+	EQ	+	+	++
Min. Megabits per full horizon (Every 500Mb diff. is +/-)	0	+++++	++++	++++++	++++++	+++	++++++
Max Operating Power (Every 0.5W diff. is +/-)	0	+	+	++	+	--	+
Total:	0	9	9	10	14	10	14
Datasheet	[6]	[7]	[8]	[9]	[2]	[10]	[11]

The ADCS-2120 Monochrome image sensor was selected over the OV7620 due to the ADCS-2120’s flight heritage aboard the CANX-1 satellite [4]. The monochrome version of the ADCS-2120 was selected to preserve the pure scientific imaging data that a color image sensor would lose when filtering the captured photons into colored pixels.

The MATLAB script ZODIphototime.m (See Appendix D.3) calculates the time it will take the ADCS-2120 to capture a single image of the zodiacal cloud, as described in Stark et. al. [5], assuming a read time of 1000s and a 10cm aperture. ZODIphototime.m calculates that it will take the ADCS-2120 sensor 2665.7099 seconds (44.4285 minutes) to capture a single image of the zodiacal cloud. For sizing and safety purposes, we round this value up and assume the ADCS-2120 sensor will take 1 hour to capture a single image. As can be seen in Table 3, it will take the ADCS-2120 sensor 232 images to capture a full horizon (incorporating a safety factor of 2). At one hour per image, this translates to 835575 seconds (9.67 days) per full horizon of images at both periapsis and apoapsis. Taking 9.67 days to image the zodiacal cloud at periapsis and apoapsis is well within the realm of feasibility for this mission. For this reason, the **ADCS-2120 Monochrome image sensor** [2] was determined to be a suitable image sensor for the Zodi CubeSat mission. The ADCS-2120 monochrome image sensor would be able to image the zodiacal cloud at both periapsis and apoapsis with high resolution, in a reasonable period of time, and with a low enough impact to the overall size of the CubeSat to ensure it remains below 6U, thereby meeting all the requirements of this mission’s scientific payload.

4.1.2 Recommendations for Future Work

Future work on the optical payload will involve a more detailed design of the telescope optical system. We currently size our optical payload by comparing it to the 1U Cassegrain optical telescope system used by the STARE pathfinder mission [3], but this remains a rough estimate until it can be confirmed that the same optical setup will work for our specific mission. At this time, there does not appear to be any reason why the optical system used by STARE could not be adapted to our system, but confirmation remains a necessary step.

Though the values used were suitable for sizing and feasibility analysis, a number of the camera parameters could use further refinement before implementation. The focal length and Mb per photo represent two areas where additional refinement would be particularly helpful.

4.2 Propulsion Subsystem

Table 5: Propulsion Subsystem Requirements for the Zodi CubeSat Mission

Requirement ID	Propulsion Subsystem Requirements	Mapping to System-Level Requirements
PRP-REQ 1	The propulsion system must execute an inclination change burn ($\sim 37.21\text{m/s}$) to achieve the desired final inclination of 9.7723 deg.	REQ 3
PRP-REQ 2	The propulsion system must execute its inclination change burn fast enough to ensure periapsis is at the proper orbital height (≤ 0.1 AU) before the CubeSat reaches periapsis.	REQ 3
PRP-REQ 3	The size of the propulsion system must be small enough to ensure that it does not put the total size of the CubeSat above 6U	REQ 1

4.2.1 Analysis

A trade study was performed on various propulsion systems in an attempt to optimize thruster volume, specific impulse, and force, in that order. Because of the single Δv requirement of 37.21m/s , the sizable time period until data collection after deployment, and an absence of a station-keeping requirement, the Busek Electro spray Thruster (BET) $100\mu\text{N}$ variant (BET- $100\mu\text{N}$) [12] and 1mN variant (BET- 1mN) [13] were selected for further analysis. These electro spray thrusters were chosen for their low dry volume, high specific impulse, high efficiency, and subsequently low fuel requirement.

Electro spray propulsion is a form of electric propulsion that produces thrust via electrostatic acceleration of droplets of charged ionic liquid (such as the 1-Ethyl-3-Methylimidazolium ionic fluid used in our propellant calculations in Appendix A). In addition to creating an electric field to accelerate this plume of charged liquid, Busek's Propellantless Field Emission Cathodes [14] also provide carbon nanotube sites for the charged plume to be neutralized, preventing a charge from being induced on the CubeSat's exterior. The primary benefits of electro spray propulsion are that it features a high specific impulse, high thrust density, and high efficiency at the cost of lower total thrust and higher power requirements when compared to chemical propulsion.

Busek's electro spray thrusters, cathodes, and valves also have the added benefit of flight heritage aboard the NASA ST-7 ESA LISA Pathfinder [15]. According to Busek's website, the "LISA Pathfinder launched from Kourou in December of 2015 and all electro spray thruster units were successfully commissions[sic] in January 2016, after having been stored, fully fueled

for nearly eight years. After reaching Earth-Sun Lagrange Point 1, the thrusters accumulated an average of 2,500 hours operation each and met 100% of mission goals"[16]. For this reason, electro spray thrusters were determined to be a suitably reliable technology for use aboard our CubeSat.

The BET-100 μ N electro spray thruster features a nominal specific impulse of 2300s, a volume 1/3 U (including electronics), a dry mass of 0.329kg, and a nominal thrust of 100 μ N. The BET-100 μ N requires 5.5W of power and an input voltage of 5.0-8.6VDC while in operation. These features of the BET-100 μ N and others are summarized below in Table 6:

Table 6: BET-100 μ N electro spray thruster product features. Pulled from Busek's BET-100 μ N Datasheet [12].

BET-100μN Electro spray Thruster	
System Power	5.5 W
Input Voltage	5.0-8.6 VDC
Interface	RS-422, RS-485
Propellant	Ionic Liquid
Cathode	Carbon Nanotube Field Emission
Thrust	100 μ N nominal
Specific Impulse	2,300 sec nominal
Delta-V	85m/s for 4kg CubeSat
Total Impulse	338 N-s (10mL propellant)
Dimensions	9cm x 9cm x 4cm
System Volume (including electronics)	1/3 U
System Dry Mass	0.329kg

The BET-1mN electro spray thruster features a nominal specific impulse of 800s, a volume 1 U (including electronics), a dry mass of 1.15kg, and a nominal thrust of 0.7mN. The BET-1mN requires 15W of power and an input voltage of 9-12.6VDC while in operation. These features of the BET-1mN and others are summarized below in Table 7:

Table 7: BET-1mN electro spray thruster product features. Pulled from Busek's BET-1mN Datasheet [13].

BET-1mN Electro spray Thruster	
System Power	15 W
Input Voltage	9-12.6 VDC
Interface	UART
Propellant	Ionic Liquid
Cathode	Carbon Nanotube Field Emission
Thrust	0.7mN nominal
Specific Impulse	800 sec nominal
Delta-V	151m/s for 4kg CubeSat
Total Impulse	605 N-s (10mL propellant)
Dimensions	9cm x 9cm x 4cm
System Volume (including electronics)	1 U
System Dry Mass	1.15kg

As can be seen in Table 6 and Table 7, the BET-100 μ N thruster features a much higher specific impulse of 2300s compared to the BET-1mN's 800s specific impulse, a lower system volume of 1/3U compared to the BET-1mN's 1U system volume, but also a much lower nominal thrust of 0.1mN compared to the BET-1mN's 0.7mN nominal thrust. For our 4U CubeSat, the BET-100 μ N thruster would be more than capable of delivering the required 37.21m/s Δv burn, but its lower thrust would require a much longer time period to execute the burn. Using the mass of our CubeSat (See Appendix A) with the propulsion system mass swapped out

according to each thruster, the time required for each thruster to execute the 37.21m/s Δv burn (assuming constant thrust) was calculated like so:

$$F_{thrust} = m \frac{\Delta v}{\Delta t}$$

$$\Delta t_{BET-100\mu N} = m \frac{\Delta v}{F_{BET-100\mu N}} = (4.39889 \text{ kg}) \frac{37.21 \text{ m/s}}{0.0001 \text{ kg m/s}^2} = 1636826.969 \text{ s} = 18.9 \text{ days}$$

$$\Delta t_{BET-1mN} = m \frac{\Delta v}{F_{BET-1mN}} = (5.225744 \text{ kg}) \frac{37.21 \text{ m/s}}{0.0007 \text{ kg m/s}^2} = 277785.6203 \text{ s} = 3.2 \text{ days}$$

According to these calculations, to execute a 37.21m/s Δv burn, the BET-100 μ N would require 18.9 days, whereas the BET-1mN would require 3.2 days.

Given the proper trajectory planning, the BET-100 μ N thruster, with its required burn time of 18.9 days, could feasibly perform the required inclination change maneuver for our CubeSat. This said, the calculated Δv burn of 37.21m/s assumed a single, impulsive burn, and the actual Δv requirement will increase as it approaches periapsis. Spending 18.9 days implementing an inclination change burn, while possible, would require much more complex simulation and control than has currently been performed in order to ensure our CubeSat still ends up in its desired final orbit. How this additional complexity and control will affect our Power and ACDS subsystems is unknown at this time and remains an area for future study.

The BET-1mN would be able to execute the calculated Δv burn of 37.21m/s in just 3.2 days. Once again, because the calculated Δv burn of 37.21m/s assumed a single, impulsive burn, the actual Δv requirement will be slightly higher, but less-so than in the BET-100 μ N case as the BET-1mN will be able to complete the burn farther from periapsis. Additionally, the higher thrust of the BET-1mN will provide greater contingency for our current trajectory and allow for greater versatility in selecting new trajectories should our current become unavailable.

Because it is, at the time of this writing, unclear as to whether the potential benefits of the BET-100 μ N's lower volume and mass would outweigh the potential additional power requirements and risk of failure associated with a 18.9 day continuous burn, the **BET-1mN Electro Spray Thruster** has been chosen as the Zodi CubeSat's propulsion system. The BET-1mN Electro Spray Thruster [13] will be able to execute the required inclination change burn of ≈ 37.21 m/s, in a reasonable period of time (3.2 days), and with an acceptable impact on the overall size of our CubeSat (1U thruster module, 0.02U propellant; See Appendix A), thereby meeting all the requirements of our propulsion subsystem.

4.2.2 Recommendations for Future Work

Additional orbital dynamics analysis should be performed with the BET-1mN incorporated into the design, and it is the opinion of this author that additional orbital dynamics analysis should also be performed on the BET-100 μ N until the additional requirements its longer burn time imposes are better understood. One goal of this orbital dynamics analysis will be to get a more accurate value for the required Δv maneuver for both the BET-1mN and the BET-100 μ N assuming a **continuous** burn, thereby allowing for their respective burn times and required propellant mass to be updated accordingly. This analysis will also provide insight into the

ACDS requirements for executing both the BET-1mN burn and the BET-100 μ N burn in such a way as to still achieve our desired final orbit, guiding the ACDS team in their feedback controller designs and helping to determine the overall feasibility of the BET-100 μ N thruster.

If this analysis determines that utilizing the BET-100 μ N will require drastic changes to the CubeSat design, impose a much higher risk than the BET-1mN, and/or if continued analysis on the BET-100 μ N would lead to unacceptable delays in the future progression of the project, then further analysis on the BET-100 μ N should be scrapped and all analysis moving forward should only include the BET-1mN. But if analysis determines that the benefit of the lower volume and mass of the BET-100 μ N outweighs its added complexity and risk, then it *may* be worth switching the propulsion system over to the BET-100 μ N, at the project team's discretion.

4.3 Communications Subsystem

Table 8: Communications Subsystem Requirements for the Zodi CubeSat Mission

Requirement ID	Communications Subsystem Requirements	Mapping to System-Level Requirements
COM-REQ 1	The communications system must transmit two full horizons worth of Zodiacal Dust images to Earth before end of life.	REQ 7
COM-REQ 2	The size of the communications system must be small enough to ensure that it does not put the total size of the CubeSat above 6U	REQ 1

4.3.1 Analysis

After collecting its final horizon of images at apoapsis, the CubeSat will pass Earth at an altitude of closest approach of 8731 km. This transmission window, and during its Earth gravity-assist represent the two best opportunities to communicate with the CubeSat. Communication via the DSN outside of these two events may be possible if emergency software updates are necessary, but obtaining time on the DSN for this purpose cannot be counted on. For this reason, all communication between Earth and the CubeSat is assumed to be made at this altitude of closest approach of 8371 km.

The CubeSat will transmit in the X-Band at 8.45GHz. The X-Band was chosen due to its high datarate capabilities and legacy for deep-space science missions. Based on the CPUT XTX X-Band Transmitter [17] and Alaris OMNI-A0150 High Gain X-Band Omni-directional Antenna [18], a link budget was assembled for both the Deep Space Network (DSN) and Near Earth Network (NEN) as potential ground receivers (See Appendix C). Based on the CPUT Transmitter datasheet, a RF power of 2W (3dBW) was chosen and the datarate was not allowed to exceed 50Mbps, keeping within the CPUT Transmitter's limits. Similarly, based on the OMNI-A0150 Antenna datasheet, an antenna gain of 4dBi was chosen based on the OMNI-A0150's limits. At this transmission frequency of 8.45GHz and distance of 8731km, the worst-case total losses were assumed to be 194.647681dB for the DSN and 197.182681dB for the NEN (See Appendix C). Our transmitter will use QPSK modulation with a 9/10 code rate, resulting in a required signal-to-noise ratio ($\frac{E_b}{N_0}$) of 3.89dB.

In order to account for uncertainty in some assumed values, a link margin of at least 3dB was chosen. For the DSN, a 40 Mbps datarate would result in a predicted $\frac{E_b}{N_0}$ of 16.242dB, a link margin of 12.352dB, and allow two horizons worth of Zodi images (≈ 2720 Mb with data redundancy of 2; See Section 4.4) to be transmitted in 68 seconds. For the NEN, a 0.392430

Mbps datarate would result in a predicted $\frac{E_b}{N_0}$ of 6.89dB, a link margin of 3dBm and allow two horizons worth of Zodi images (≈ 2720 Mb; See Section 4.4) to be transmitted in 6931.17 seconds (1.93 hours).

Of our two analyzed ground stations (the DSN and NEN), the NEN is far more likely to be our final ground station, due to the high demand and cost of the DSN. The 1.93 hour transmission time that would result from the 0.392430 Mbps transmission datarate to the NEN is perfectly feasible, and could be further improved if link margins below 3dB are allowed. Additionally, the high 16.242dB link margin that would result from using the DSN as a ground station suggests that transmission could begin at distances much farther than the 8371km altitude of closest approach if the DSN is used. Both of these results prove the feasibility of using an X-Band transmitter and omni-directional antenna like the **CPUT XTX Transmitter** and **Alaris OMNI-A0150** for our Zodi CubeSat. The CPUT XTX Transmitter [17] and Alaris OMNI-A0150 Antenna [18] would be able to transmit all scientific data to the NEN in a reasonable period of time (1.93 hours), retain a 3dB link margin as they do so, and with an acceptable impact on the overall size of our CubeSat (0.092U transmitter, 0.046U antenna; See Appendix A), thereby meeting all the requirements of our communications subsystem.

4.3.2 Recommendations for Future Work

Though the values used were suitable for sizing and feasibility analysis, where possible the link budget should be further refined. More accurate values for losses as well as specific target ground stations (rather than just sizing for the worst ground station in each network) would improve our link budget and likely our maximum datarate by extension. A better understanding of the specific losses and ground stations that our CubeSat will encounter will allow us to confidently lower our required link margin and raise our maximum datarate.

The costs and availabilities of both the DSN and NEN ground stations should be looked into as the project progresses. From this, the final feasibility of using the DSN as a primary or emergency ground station can be determined. Additional analysis should be performed incorporating the relative positions of the Earth and CubeSat to determine available contact windows using the DSN in the event an emergency software update is necessary.

Additional work should also be done to assemble an uplink link budget to compliment the downlink link budget provided in Appendix C. The downlink link budget was assembled using the CPUT XTX transmitter as a reference, so further research should also be done to find a similar or superior transceiver should the CPUT XTX be incapable of receiving data.

4.4 Command & Data Handling Subsystem

Table 9: C&DH Subsystem Requirements for the Zodi CubeSat Mission

Requirement ID	Command & Data Handling Subsystem Requirements	Mapping to System-Level Requirements
CDH-REQ 1	The C&DH system will ensure the CubeSat accomplishes all mission goals autonomously and without computational error due to cosmic radiation.	REQ 2 REQ 5
CDH-REQ 2	The C&DH system will ensure that all collected data is stored and protected from corruption due to cosmic radiation.	REQ 6
CDH-REQ 3	The size of the C&DH system must be small enough to ensure that it does not put the total size of the CubeSat above 6U.	REQ 1

4.4.1 Analysis

Our CubeSat will use triple modular redundancy (TMR) to ensure the mission is executed autonomously and without faults once it has been deployed. TMR is the process by which three identical systems run the same identical processes and execute a final command based on majority consensus, thereby protecting the system logic from bit flip errors caused by cosmic radiation. This TMR system will be comprised of three micro-controllers. For sizing we used three Raspberry Pi Model 3B+'s as a reference. This Raspberry Pi TMR would require only 3.6W to operate [19].

The C&DH system will also be responsible for ensuring all the collected scientific data is stored without error until it can be transmitted back to Earth. As mentioned previously, a horizon of photos would be approximately 680Mb of data in their uncompressed form (See Section 4.1). Because our CubeSat will collect images from both periapsis and apoapsis, raw image data will take up 1360 Mb of data storage. To protect this data against bit flip faults caused by cosmic radiation, a data redundancy of 2 will be applied (system will store 2 copies of all scientific data), resulting in a total 2720 Mb of image data. A small, 5 Gb solid-state harddrive would be able to feasibly store this collected data as well as any algorithms the CubeSat will need to operate autonomously.

Using this configuration, the C&DH subsystem will feasibly be able to ensure the Zodi CubeSat can operate autonomously, store all collected scientific data without errors, and have minimal impact on the overall size of our CubeSat, thereby meeting all the requirements of the C&DH system.

4.4.2 Recommendations for Future Work

The primary focus of future C&DH work will involve the design of the CubeSat's autonomous operation algorithms. These algorithms are **mission critical**, as the CubeSat will need to work autonomously and reliably at the distances outside of communication range, where opportunities to diagnose and fix software problems will be extremely limited or potentially nonexistent. Additional work is to be done on the design and implementation of both the hardware and software of the TMR system. Additional research into potential micro-controllers should also be performed to ensure they will be able to operate at the temperatures that our CubeSat will be exposed to (See Section 4.7).

4.5 Power Subsystem

Table 10: Power Subsystem Requirements for the Zodi CubeSat Mission

Requirement ID	Power Subsystem Requirements	Mapping to System-Level Requirements
PWR-REQ 1	The power subsystem will ensure that sufficient power is provided to all necessary CubeSat hardware until end of life in order to facilitate the completion of the mission.	REQ 5 REQ 7
PWR-REQ 2	The size of the power subsystem must be small enough to ensure that it does not put the total size of the CubeSat above 6U.	REQ 1

4.5.1 Solar Array Analysis

The CubeSat will feature body-mounted and deployable Triple-Junction GaAs solar arrays using the AzurSpace Triple-Junction GaAs solar cell [20] as a reference. This solar array will provide a total sun-incident surface area of 1200cm^2 (0.12m^2) and will be able to provide power to all subsystems even when operating at maximum power. The sizing derivation for this solar array is as follows.

Based on the maximum power requirements from our power budget (See Appendix B), the CubeSat will require 25W while executing its inclination change, 10.2W while imaging the zodiacal cloud, 10W while in transit/standby between mission events, and 25W while transmitting data to Earth. For sizing purposes, these values assume the overestimated case of all utilized hardware operating at its maximum wattage while in use.

The "Solar Panel Power Generation" section of ZODItrajectory.m (See Appendix D.1) derives the end-of-life (EOL) power that would be generated by 1200cm^2 worth of Silicon, GaAs, and Triple-Junction GaAs solar cells between orbit insertion/periapsis, periapsis/apoapsis, and apoapsis/Earth-transmission. These EOL power generation values are generated assuming an incidence angle of 9.7725° (inclination of orbit), a beginning-of-life (BOL) inherent degradation of 0.7225 (that is, the degradation will cause the cell to generate 72.25% of intended power), a Triple-Junction GaAs cell efficiency of 0.28, a GaAs cell efficiency of 0.185, and a Silicon cell efficiency of 0.148.

EOL degradation due to radiation is estimated according to the 1MeV particle fluences estimated by ZODIpanelDegradation.m (See Appendix D.2), using the NASA GaAs Radiation Handbook [21] as a guide. ZODIpanelDegradation.m makes the rough assumption that the CubeSat will experience 3 worst-case solar events at every energy range based on historically recorded maximum-energy solar event data. This is likely a gross overestimation of the actual solar fluences the CubeSat will experience. ZODIpanelDegradation.m further overestimates the damage that will be caused by solar events by taking degradation values for solar cells with no cover glass (the Zodi CubeSat solar array will likely have cover glass). By sizing our panels according to these overestimations, we hope to protect our solar array from errant high-energy solar events as well as incorporate temperature degradation due to the high temperatures the panels will reach at periapsis (See Section 4.7). Using this model, ZODIpanelDegradation.m estimates a total solar 1MeV fluence of $2.383\text{e}15$ particles per cm^2 over the lifetime of the CubeSat. This maps to a power degradation of 0.85 according to the AzurSpace Triple-Junction GaAs Solar Cell Datasheet [20] and a power degradation of 0.85 according to the Spectrolab Ultra-Triple-Junction GaAs Cell Datasheet [22], but due to the imprecise nature of ZODIpanelDegredation.m, an EOL degradation value of 0.80 was chosen for extra safety.

The absolute worst-case scenario would be if a high-energy solar event occurs while the CubeSat is at periapsis. This is modeled in ZODIpanelDegradation.m as 1 worst-case event at every energy level occurring when the CubeSat is closest to the sun at periapsis. If this occurs, the CubeSat will be subjected to $1.211\text{e}15$ particles per cm^2 **per minute**. This will not only kill the solar panels, but likely any electronics within the CubeSat. Due to the CubeSat's small size, there is unfortunately little that can be done to shield the craft from this event should it occur. Luckily, solar events of this magnitude only occur very infrequently during solar maximum, so ensuring the CubeSat will reach periapsis outside of solar maximum will reduce this risk astronomically. Even in the event where launching outside of solar maximum is impossible, these high-energy solar events are significantly rare, so the probability of one occurring while

the CubeSat is at periapsis is extremely low. Ultimately, because of the unpredictable nature of when solar events will occur, the lack of methods available to protect a CubeSat from it, and the relative low cost of a CubeSat, it is the opinion of this author that future Zodi mission designers keep this worst-case scenario in mind, but not let it drive mission-critical decisions.

With BOL and EOL degradation values obtained, ZODItrajectory.m calculates the solar flux incident on the CubeSat at each point in its orbit, and from this calculates the power generated by each type of solar array assuming EOL power generation throughout. In the "Battery & Solar Panel Sizing" section of ZODItrajectory.m, the script goes on to determine the minimum number of 10x10cm panels necessary to make batteries unnecessary, assuming no eclipse. Inspecting the trajectory indicates that the CubeSat will be positioned between the Earth and Sun during transmission, and therefore will not be eclipsed by the Earth during this time, thus this is a reasonable assumption. These values are output by the script and shown below in Listing 2:

```

Power Used In Transit (Standby): 10 W
Number of 10x10cm Solar Panels: 12

Power Generated In Transit:
5   Power Generated Before Periapsis:
    Triple Junc GaAs: 167822634.7321 W*s
    GaAs: 90817937.716 W*s
    Si: 60826634.6677 W*s

10  Power Generated Between Periapsis and Apoapsis:
    Triple Junc GaAs: 252738384.9306 W*s
    GaAs: 116286128.669 W*s
    Si: 63141565.704 W*s

15  Power Generated Between Apoapsis and Earth Transmission:
    Triple Junc GaAs: 84747100.864 W*s
    GaAs: 25388039.9868 W*s
    Si: 2269247.8557 W*s

20  Minimum Number of 10x10cm (TripleGaAs) Solar Panels to Make Batteries Unnecessary: 10.1339
    Minimum Number of 10x10cm (GaAs) Solar Panels to Make Batteries Unnecessary: 15.3379
    Minimum Number of 10x10cm (Si) Solar Panels to Make Batteries Unnecessary: 19.1723
    Number of 10x10cm Solar Panels: 12

25  Minimum LiIon Battery Volume: -7.4489e-05 m^3 = -0.074489U (assuming TripleGaAs Solar Cells
    ↪ )
    Minimum NiCd Battery Volume: -0.0001243 m^3 = -0.1243U (assuming TripleGaAs Solar Cells)
    Minimum NiH2 Battery Volume: -0.00031577 m^3 = -0.31577U (assuming TripleGaAs Solar Cells)

```

Listing 2: Output of the "Solar Panel Power Generation" and "Battery & Solar Panel Sizing" sections of the ZODItrajectory.m MATLAB script. Negative "Minimum Battery Volume" values indicate that the solar array would be able to provide power balance without a battery. See full ZODItrajectory.m script in Appendix D.1

The script also plots the power that would be generated by each type of 1200cm^2 solar array as a function of time, as shown in Figure 5:

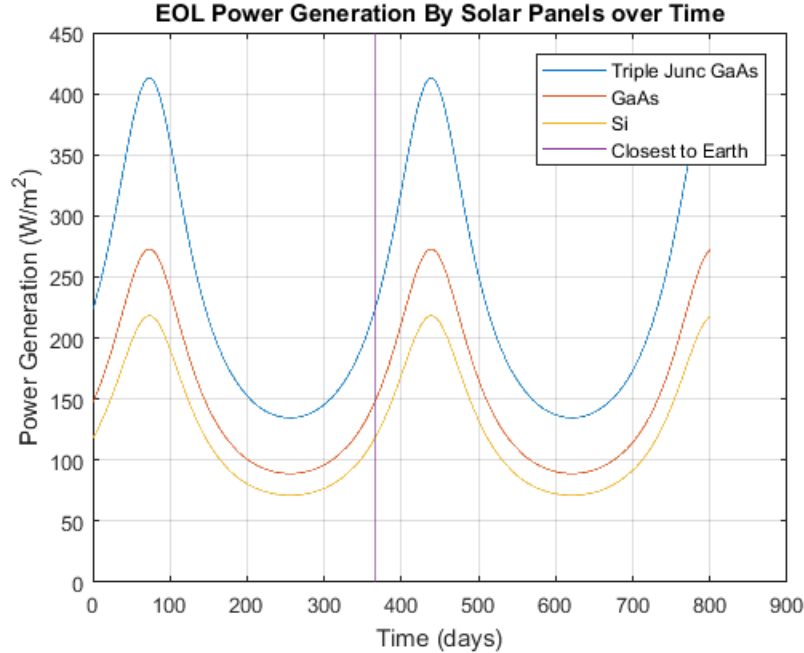


Figure 5: Plot of power generated by a $1200cm^2$ sun-incident Triple-Junction GaAs, GaAs, and Silicon type solar array. Plot generated by ZODItrajectory.m MATLAB script. See full ZODItrajectory.m script in Appendix D.1.

Thus it was determined that a $1200cm^2$ Triple-Junction GaAs solar array would be able to provide power to the Zodi CubeSat at all mission stages, even with all hardware operating at maximum wattage. A battery would not be necessary to provide power to the system, but our power subsystem still features a 1/3U Li-Ion battery for safety purposes (See Section 4.5.2 for more details). Therefore, we have concluded that the Zodi CubeSat could feasibly operate with a combination of body-mounted and deployable solar arrays (See CAD model in Figure 1) made up of Triple-Junction GaAs cells like the **AzurSpace Triple-Junction GaAs Cell** [20]. This power subsystem would safely power the Zodi CubeSat for the duration of its mission and would not impact the overall size of the CubeSat such that it exceeds 6U (See Appendix A), thereby meeting all of its subsystem requirements.

4.5.2 Battery Sizing Analysis

The "Battery & Solar Panel Sizing" section of ZODItrajectory.m calculates the battery volume that would be required to provide power balance for a given solar array surface area. The script performs this analysis for Li-Ion, Ni-Cd, and Ni-H₂ batteries. As mentioned previously in Section 4.5.1, the solar array of the Zodi CubeSat is sized such that the solar array alone will be able to provide power to all hardware at all stages in the mission. For safety, however, the CubeSat will contain a 1/3U Li-Ion battery. This battery will be able to act as a bridge between the solar arrays and the rest of the CubeSat hardware, provide power to the CubeSat hardware in the event of incomplete solar array deployment, provide power in the event of solar eclipse, and provide internal heating to the CubeSat at apoapsis. A fully charged 1/3U Li-Ion battery with a volumetric energy density of 250Wh/L would be able to provide 83.333 Wh of power. This would help cover some or even all of the power deficit caused by a partially-deployed solar array wing.

The only points at which our CubeSat's view of the sun may become eclipsed are during

its final Earth gravity-assist (eclipsed by the Earth) and possibly while it is transmitting its scientific data one year later (eclipsed by the moon). In the former case, the battery will be able to provide 8 hours of power while the CubeSat operates in standby (10W used in standby; See Appendix B), ensuring the CubeSat remains powered until it has passed the Earth. In the later case, the power requirement will be higher due to data transmission. Based on our link budget (See Appendix C), the longest required time to transmit all collected data would be approximately 1.93 hours. This means that, should the sun be eclipsed by the moon during transmission, a fully charged 1/3U Li-Ion battery would be able to provide 43.28 W for the duration of the transmission time. Considering that the CubeSat will require a maximum of 25W (See Appendix B) during transmission, the power provided by this Li-Ion battery would be more than enough even after factoring in a year's worth of degradation and duty-cycling.

For this reason, a 1/3 U Li-Ion battery would feasibly be able to provide power to the Zodi CubeSat even in the event of solar array deployment failure and/or a solar eclipse, thereby ensuring the CubeSat will remain powered in all stages of its mission. As an added bonus, the battery will generate heat and warm the interior of the CubeSat when it is at its coldest at apapsis. For more thermal analysis concerning the battery, see Section 4.7.

4.5.3 Recommendations for Future Work

The power subsystem was sized using a number of overestimations to ensure it would be able to meet the requirements of the system. As a result of this, however, the power subsystem is likely larger than it actually needs to be in order to fully power all hardware on the CubeSat. Further refinement of the power subsystem should be done in the future in order to optimize the sizing of both the solar array and backup battery.

Though the values used were suitable for sizing and feasibility analysis, the solar array degradation calculations are particularly in need of refinement. As is, solar array degradation due to radiation is very roughly estimated assuming a specific number of events. A more proper and accurate method of quantifying the solar radiation that a spacecraft will encounter is to make a probabilistic model and select an expected total particle fluence value based on a probabilistic confidence value (of 90% for example). Additionally, solar array and battery degradation due to temperature need to be incorporated, especially for the deployable solar panels that will reach temperatures of up to 137.49°C at periapsis (See Section 4.7).

The current power subsystem design will require some level of regulated power bus due to the Li-Ion battery, but future analysis may allow for the system to be simplified to an unregulated configuration. Whether or not this simplification would actually add any value to the system, however, has not been meaningfully explored. In the case of a regulated power bus, this system will need to be designed in a way that makes the most sense for the Zodi CubeSat and its mission.

4.6 Attitude Control & Determination Subsystem

Table 11: ACDS Subsystem Requirements for the Zodi CubeSat Mission

Requirement ID	Attitude Control & Determination Subsystem Requirements	Mapping to System-Level Requirements
ACDS-REQ 1	The ACDS system must be able to determine the CubeSat's position & orientation in space	REQ 2
ACDS-REQ 2	The ACDS system must be able to orient the CubeSat in any direction in 3D space.	REQ 2 REQ 3
ACDS-REQ 3	The ACDS system must be able to precisely point the CubeSat camera while it images the Zodiacal cloud	REQ 4
ACDS-REQ 4	The ACDS system must be able to counteract any sources of external torque without saturating its momentum wheels to ensure consistent attitude control until end of life.	REQ 5
ACDS-REQ 5	The size of the ACDS system must be small enough to ensure that it does not put the total size of the CubeSat above 6U.	REQ 1

4.6.1 Attitude Determination Analysis

Orbital positioning will be provided by a sun sensor and star tracker due to the CubeSat's operation in deep space. An internal gyroscope will provide gyroscopic data to the Attitude Control system. If necessary, our scientific payload camera may be able to act as a star-tracker when not collecting scientific data by using an image-recognition algorithm, though a separate star tracker would be preferable to allow for orbital positioning determination during scientific data collection.

This setup would feasibly allow our Zodi CubeSat to determine its position on its orbital trajectory as well as its orientation in space, thereby meeting all the requirements of the attitude determination subsystem.

4.6.2 Attitude Control Analysis

The CubeSat will use a feedback controller hooked up to a 4-Wheel Reaction Wheel Assembly (RWA), using 4 Blue Canyon RWP050 Reaction Wheels [24] as a reference. The CubeSat will use cold-gas thrusters with RC134a propellant ($I_{sp}=40$) to dump momentum and prevent reaction wheel saturation. This attitude control assembly was deemed suitable after sizing the sweeping angle, maximum angular rate, and external torque imparted by solar radiation pressure.

Attitude control subsystem sizing was handled by the "Attitude Control System Sizing" section of ZODItrajectory.m (See Appendix D.1). This section of the script determines the maximum angular rate, max sweeping angle, and the change in momentum due to solar radiation pressure during image collection. Using this data, it determines the number of momentum dumps and mass of cold-gas fuel that will be required to dump all accumulated momentum in the CubeSat's lifetime.

The angular rate of the CubeSat will be highest operationally when the CubeSat needs to dwell on a single point. This occurs at both periapsis and apoapsis while the Camera is imaging the Zodi cloud. The required angular rate will be higher at periapsis due to the higher orbital velocity of the CubeSat, peaking when imaging precisely at periapsis. Using the ZODItrajectory.m script, it was determined that at periapsis the CubeSat will need to sweep

8.35067e-4 rad, resulting in a maximum angular rate of 3.62332e-7 rad/s. This is well within the capabilities of our proposed reaction wheel assembly. The script also determined that the CubeSat will need to sweep a total of 0.3 rad at periapsis and a total of 0.0991 rad at apoapsis while imaging the Zodi cloud.

After the CubeSat is deployed and leaves Earth's sphere of influence, until its next Earth flyby the only possible source of external torque will be solar radiation pressure. We make the assumption that while in transit, the CubeSat will be made to spin such that forces imparted by solar radiation pressure will cancel out. Using this assumption, the external torques for which our attitude control system must be sized will occur during photo collection at periapsis and apoapsis, where the CubeSat must stop spinning. We assume a worst-case scenario of a 10cm distance, D , between the CubeSat's center of mass and the center of incident solar radiation pressure. Because the exterior of our CubeSat is covered in solar arrays with an absorptivity of 0.91 [20], the reflectance of our CubeSat exterior is calculated to be $R = \frac{1}{10^a} = \frac{1}{10^{0.91}} = 0.1230$. Using this value, the instantaneous change in momentum due to solar radiation pressure was calculated like so:

$$\Delta M_{SRP} = \frac{\Phi_S(t)}{c}(A)(1 + R)(D)(\Delta t) \cos \theta$$

Where $\Phi_S(t)$ is the solar flux at time t , c is the speed of light (3e8 m/s), A is the surface area on which the sunlight will be incident, R is the reflectance, D is the distance between the center of mass and center of incident solar radiation pressure, Δt is the time over which the CubeSat will be exposed to these conditions, and θ is the angle of the incident surface with respect to the incoming sunlight. For our calculations, the total change in momentum was calculated for the entire duration of image collection at periapsis and apoapsis taking $D = 0.1 \text{ m}$ (as mentioned previously), $A = 0.12 \text{ m}^2$ (the total area of solar panels incident to the sun), $R = 0.1230$ (as mentioned previously), $\theta = 9.7723^\circ$ (inclination angle), $\Delta t = 2304.699 \text{ s}$ (the time between two datapoints), and $\Phi_S(t)$ calculated for each datapoint during which images will be collected.

Using these parameters, it was determined that the total combined change in momentum that will occur at periapsis and apoapsis will be 0.1277 Nms. Taking the maximum momentum storage of each our 4 wheels to be 0.050 Nms (as described in the Blue Canyon RWP050 Datasheet [24]) and incorporating a safety factor of 1.2, this would result in our wheels reaching 76.62% saturation before end of life. This is well within acceptable limits. Nevertheless, to account for possible momentum imparted by the Earth and during deployment, a momentum dumping system was sized to remove the 0.1277 Nms that solar radiation pressure will impart.

As stated previously, our momentum dumping system consists of cold-gas thrusters using RC134a propellant. RC134a propellant has a specific impulse of 40 s. Assuming a 1 second burn time, incorporating a safety factor of 1.5 and assuming 10cm to be the largest moment arm distance for our thrusters, the total fuel required for our momentum dumping system was calculated as follows:

$$F_{MomentumDump} = \frac{\Delta M_{tot}}{(r_{moment \ arm})(t_{burn})}(X_{Safety}) = \frac{0.1277 \text{ Nms}}{(0.1 \text{ m})(1 \text{ s})}(1.5) = 1.916 \text{ N}$$

$$m_{RC134a} = (F_{MomentumDump}) \frac{N_{MomentumDumps}}{(g)(I_{sp})} = (1.916 \text{ N}) \frac{0.7662}{(9.80665 \text{ m/s}^2)(40 \text{ s})} = 0.0037418 \text{ kg}$$

Where $N_{MomentumDumps}$ is the number of times that the wheels must be completely dumped

of momentum (0.7662 because they only reach 76.62% saturation), and g is the gravitational constant (9.80665 m/s^2).

Using the atmospheric density of RC134a, 4.25 kg/m^3 , a 5000 psia pressure tank, and Boyle’s law, it was determined that this 0.0037418 kg of RC134a would translate to 2.588 cm^3 (0.00259 U) in volume, not counting its storage tank (See Mass-Vol Budget in Appendix A). This volume is more than acceptable and this cold-gas system would be able to dump all momentum imparted by solar radiation pressure, ensuring our system will be able to survive to end of life without wheel saturation. Based on this analysis, we can conclude that 4 reaction wheels similar to the **Blue Canyon RWP050** [24] and a cold-gas thruster array using RC134a fuel would provide feasible attitude control to our Zodi CubeSat. This attitude control system would be able to provide the necessary pointing slew rate, perturbation resistance, prevent wheel saturation, and do so with an acceptable impact on the overall size of the CubeSat, thereby meeting all attitude control subsystem requirements.

4.6.3 Recommendations for Future Work

The primary focus of future ACDS analysis will be the creation of a feedback controller for the ACDS system. To do this, a working inertia matrix will need to be determined based on the final design configuration of the CubeSat. Determining the actual position of the CubeSat’s center of mass would be necessary for accurate attitude control and calculation refinement. Though the momentum values used were suitable for sizing and feasibility analysis, further refinement of the expected change in momentum would be beneficial, as would determining the required rotational dynamics during transit to ensure no net momentum is imparted.

Another area of future analysis would be the optimization of reaction wheel and momentum dumping thruster placement. Currently, the reaction wheel assembly is represented in the CAD model as a box (See Figure 2), and our CubeSat features far more momentum-dumping thrusters than are actually necessary, with 3 thrusters at each corner. The final positions and orientations of these reaction wheels and momentum-dumping thrusters should be optimized and finalized before the final assembly.

4.7 Thermal Analysis

Table 12: Thermal Subsystem Requirements for the Zodi CubeSat Mission

Requirement ID	Thermal Subsystem Requirements	Mapping to System-Level Requirements
THM-REQ 1	The CubeSat must be designed such that the maximum and minimum temperature tolerances of its components are not exceeded such that the CubeSat is unable to complete its mission.	REQ 5
THM-REQ 2	The CubeSat shall regulate its temperature passively without the need for additional heaters or radiators.	REQ 5 REQ 1

4.7.1 Analysis

A finite element thermal analysis was performed in ANSYS for our CubeSat. Heat transfer via conduction across all components and radiation into/out of the exterior components was modeled. Internal radiation and internal heat sources were not modeled. The solar panels and camera lens on the exterior of the CubeSat were modeled as plexiglass with a thermal

conductivity of 0.200 W/(mK) and an emissivity of 0.85, while all other components were modeled as an aluminum alloy with thermal conductivity according to Figure 6 as a function of temperature [25].

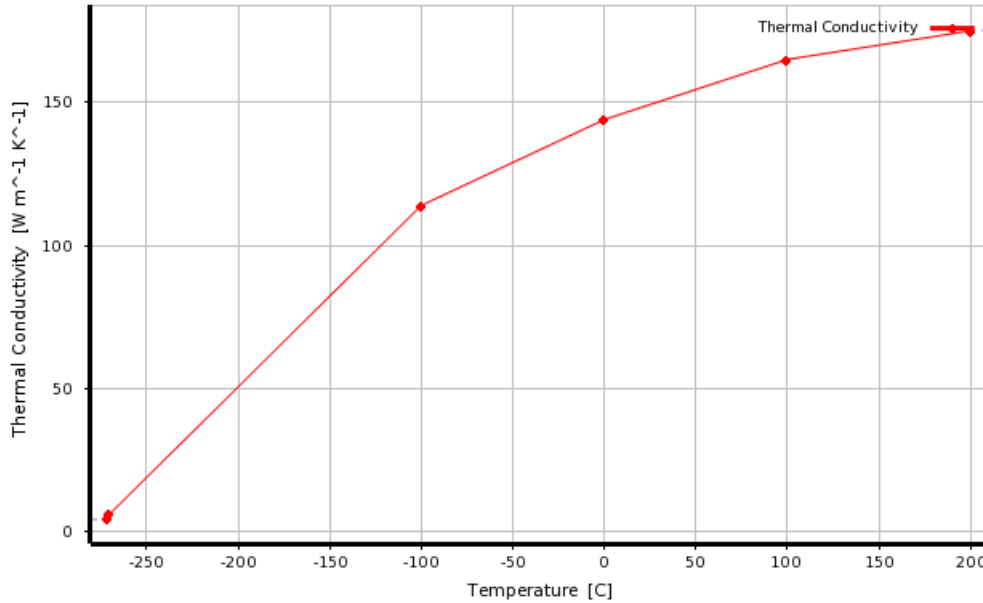


Figure 6: Thermal conductivity profile of Aluminum Alloy based on the results of Barucci et. al. [25] for temperatures below -100° . For temperatures above -100° , the standard "Aluminum Alloy" ANSYS profile was used.

A simulation was performed for the case of sunlight fully incident on one side of the CubeSat while at periapsis, representing the point at which our CubeSat will achieve its highest temperature. At periapsis, the CubeSat will be 108748530.4715 km from the sun and solar flux will be equal to $2588.8W/m^2$. The sun-facing side will be covered in solar cells with absorptivities of 0.91 [20]. To represent this, the sun-facing side was modeled as having an incident heat flux of $2355.808W/m^2 (= (0.91) * (2588.8W/m^2))$. Applying these parameters in ANSYS to the CubeSat CAD Model in Figure 1 produced the following temperature distribution at periapsis, shown below in Figure 7:

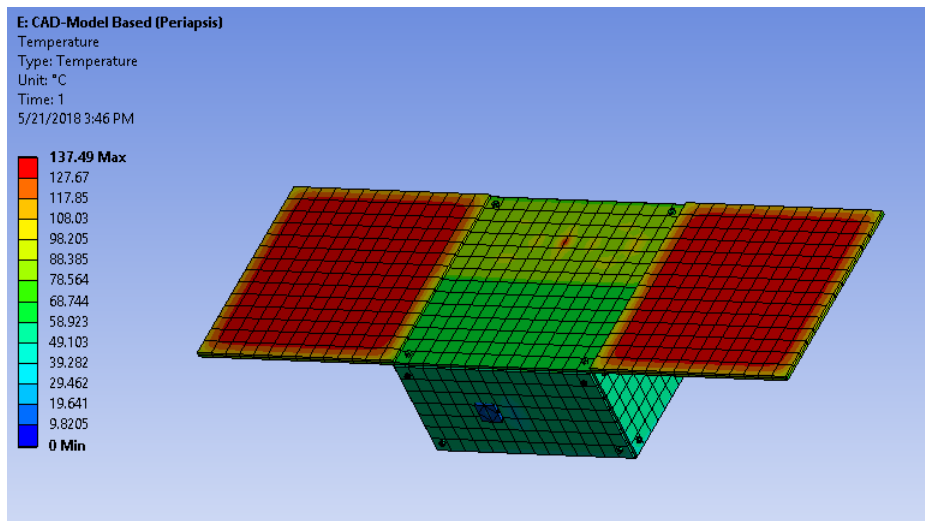


Figure 7: Temperature distribution for our CubeSat at **periapsis**. Generated using ANSYS.

This temperature model indicates that at periapsis, the majority of the CubeSat will be between the temperature range of 50–100°C (with the exception of the deployed panels which will reach temperatures of 137.49°C).

A similar analysis was performed for the case of sunlight fully incident on one side of the CubeSat while at apoapsis, representing the point at which our CubeSat will achieve its lowest temperature. At apoapsis, the CubeSat will be 190397164.4198 km from the sun and solar flux will be equal to $844.556W/m^2$. Like before, the sun-facing side will be covered in solar cells with absorptivities of 0.91 [20]. To represent this, the sun-facing side was modeled as having an incident heat flux of $768.55W/m^2 (= (0.91) * (844.556W/m^2))$. Applying these parameters in ANSYS to the CubeSat CAD Model in Figure 1 produced the following temperature distribution at apoapsis, shown below in Figure 8:

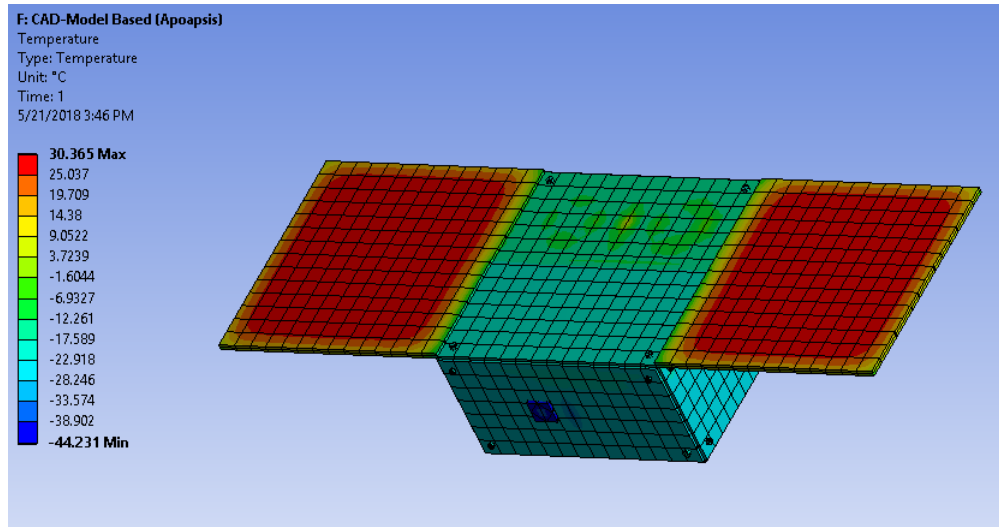


Figure 8: Temperature distribution for our CubeSat at **apoapsis**. Generated using ANSYS.

This temperature model indicates that at apoapsis, the majority of the CubeSat will be between the temperature range of -30–0°C (with the exception of the deployed panels which will reach temperatures of 30.365°C).

A significant area of interest in this analysis is the temperature of the battery. Our CubeSat uses a Lithium Ion battery, which is sensitive to extreme temperatures. A typical Li-Ion battery is designed to safely charge in the 0–45°C temperature range and discharge in the -20–60°C temperature range. Certain specialty Li-Ion batteries do exist that can safely operate outside of this range by a factor of $\pm(5 - 10)^\circ\text{C}$. A temperature probe was placed on the battery in both of our ANSYS models to determine the average steady-state temperature of our battery in the lowest and highest temperature cases (apoapsis and periapsis).

At periapsis, our battery reached a steady-state average temperature of approximately 60°C, as shown in Figure 9. This is towards the upper limit of the Li-Ion maximum discharge range, but still within feasible limits for a lithium ion battery with higher temperature tolerances. Charging while at periapsis will be unnecessary, as at this distance the solar array alone will be enough to supply power to all subsystems. Because of this, being outside the charging temperature tolerance should not be an issue. In the unlikely event that the Li-Ion battery must discharge to supply some additional power at periapsis, a lithium-ion battery with a slightly higher temperature tolerance will be able to handle this situation without incident. Incorporating internal radiation and internal temperature sources will likely change this resulting

temperature, so further analysis is necessary, but with proper power regulation this should not affect the battery temperature at periapsis by more than a few degrees.

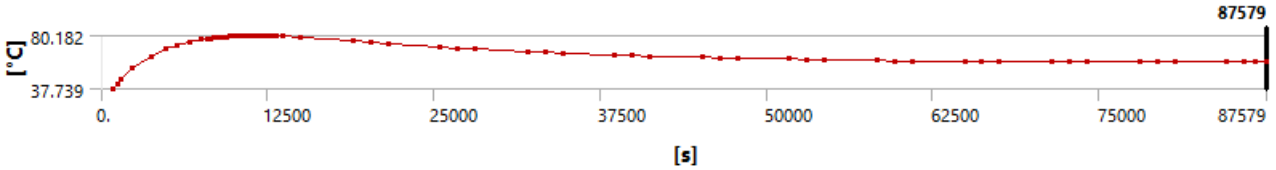


Figure 9: Transient temperature of battery over the course of one day at **periapsis**. The initial jump seen in the plot is due to the model adjusting from the arbitrary initial temperature of 22°C. The section of the plot where the temperature levels out represents the steady-state temperature of approximately 60°C. Generated using ANSYS.

At apoapsis, our battery reached a steady-state average temperature of approximately -20°C, as shown in Figure 10. This is below the minimum charging temperature for Li-Ion batteries but above the minimum discharge temperature. In the case of apoapsis, incorporating internal radiation and internal temperature sources into our model will have a much greater effect on our system. The heat generated by the battery alone will likely raise the battery temperature by several degrees, potentially putting it above the minimum charging temperature. The use of lithium-ion batteries with a lower temperature tolerance would further assist in getting the temperature of the battery into the charge range. Regardless of whether or not the battery will achieve an effective charging temperature, however, the solar panels were sized to be able to provide enough power to all subsystems even at apoapsis. Because of this, at the only potential need for the battery at apoapsis would be discharging to supply power, which it is already within the temperature range to do.

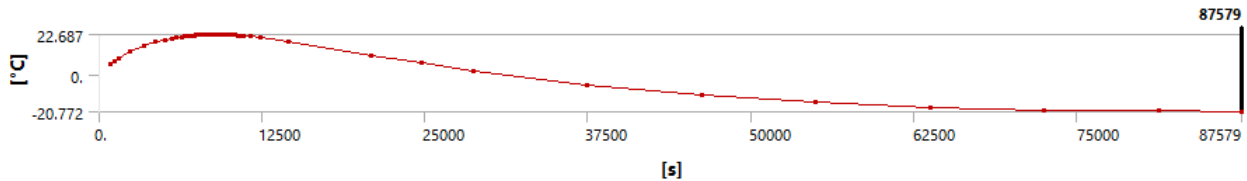


Figure 10: Transient temperature of battery over the course of one day at **apoapsis**. The initial jump seen in the plot is due to the model adjusting from the arbitrary initial temperature of 0°C. The section of the plot where the temperature levels out represents the steady-state temperature of approximately -20°C. Generated using ANSYS.

From this analysis, we can conclude that the internal temperature of our CubeSat will be such that it does not exceed the maximum or minimum operating range of our most temperature-sensitive components. Additional refinement of the model and incorporation of additional thermal coatings into the CubeSat design will bolster the feasibility of the thermal subsystem even further. For this reason, we can conclude that the thermal subsystem, as designed, would be feasible and meet all thermal subsystem requirements.

4.7.2 Recommendations for Future Work

Further thermal analysis should be performed. This additional thermal analysis should include internal radiation as well as internal heat sources, such as the CPU and battery. The thermal properties of the various CubeSat components should be further refined according to the final design of the CubeSat. Additionally, more research should be performed in order to determine the best coatings use for the interior and exterior components in the CubeSat's final

design in order to achieve the optimal temperature conditions. The ANSYS model should be updated as the design is updated.

4.8 Structure

Table 13: Structural Requirements for the Zodi CubeSat Mission

Requirement ID	Structure Subsystem Requirements	Mapping to System-Level Requirements
STRC-REQ 1	The CubeSat structure must house all hardware within a standard CubeSat configuration no larger than 6U.	REQ 1
STRC-REQ 2	The CubeSat structure must be able to withstand the gravitational, thermal, and vibrational loads associated with launch from within its deployment pod.	REQ 5
STRC-REQ 3	The CubeSat structure must be able to withstand the thermal loads it will encounter post-launch for the duration of its mission until end of life.	REQ 5
STRC-REQ 4	The CubeSat structure must be such that the deployment of any/all deployables does not cause any resonant frequencies to be achieved.	REQ 5

4.8.1 Analysis

As stated previously, the structure of our CubeSat will be a standard 4U CubeSat frame in a 20cm x 20cm x 10cm configuration. The 0.745 kg mass of this structure (See Appendix A) was derived from the combination of four modular ISIS CubeSat Structures [26]. This 4U configuration will allow the CubeSat to be deployed using a properly sized CubeSat deployment pod. Until the final design configuration of the Zodi CubeSat is finalized, more in-depth structural-dynamics analysis cannot occur. Because of the standardized nature of CubeSat structures, however, we foresee no reason why this 4U CubeSat will have any difficulties meeting its structural requirements. For this reason, the structure of our CubeSat had been determined to impart no negative impact on the feasibility of the Zodi mission.

4.8.2 Recommendations for Future Work

Once the final Zodi CubeSat design is finalized, in-depth structural-dynamics analysis will be required to ensure that the CubeSat survives the gravitational, thermal, and vibrational loads of launch from within its deployment pod. This structural analysis will also need to model solar array deployment and ensure no resonant frequencies are achieved because of it. A third objective of this structural analysis would be to ensure the CubeSat materials do not deform due to the thermal loads it will encounter on its close approach to the Sun. Additionally, because of the limited volume, it will likely not be possible to incorporate meaningful structural radiation shielding, though this possibility is still worth exploring.

5 Conclusions

Based on the performed analyses, we can confidently conclude that a 4U CubeSat mission to image the zodiacal dust cloud from above the ecliptic would be highly feasible. The BET-1mN electro-spray thruster [13] will be able to perform the necessary Δv burn to achieve the desired periapsis orbital height of 0.1283AU and apoapsis orbital height of 0.2215 after an Earth gravity assist, while only taking up 1U of volume. An ADCS-2120 monochrome image sensor [2] and Cassegrain optical telescope setup [3] will be able to completely image the zodiacal dust cloud at both periapsis and apoapsis in just 9.67 days, with high resolution, and while taking up only 1U of volume. A triple modular redundancy control system comprised of 3 micro-controllers like the Raspberry Pi Model 3B+ [19] will be able to operate the CubeSat autonomously, and all scientific data could be redundantly stored on a 5Gb solid state drive. Four Blue Canyon RWP050 reaction wheels [24] will be able to orient the CubeSat with a fast enough slew to properly collect its images, cancel out the external torques resulting from solar radiation pressure, and do so without ever reaching wheel saturation. A cold-gas RC134a momentum-dumping system requiring only 3.7g of fuel will be able to dump all the momentum stored as a result of solar radiation pressure, ensuring that the CubeSat will retain attitude control even if it experiences unexpected external torques. A 1200cm^2 triple-GaAs solar array [20] will be able to fully power the CubeSat at all stages of its mission, even with all hardware operating at maximum wattage. The CubeSat will be able to power itself even during eclipse and partial solar array deployment by housing a 1/3U Li-Ion battery. Thermal analysis confirms that the battery (the most temperature-sensitive hardware on the CubeSat) will be able to continue operating under the maximum and minimum expected temperatures. An OMNI-A0150 X-Band omni-directional antenna [18] and CPUT X-Band transmitter will be able to transmit all scientific data in a reasonable transmission time of 1.93 hours using the NEN or 68 seconds using the DSN. Finally, the Zodi CubeSat will be able to do all of this and still achieve a final volume of just 3.89 U.

It is the opinion of this author at the time of this writing that the Zodi CubeSat Project is ready to move past feasibility analysis, and onto practical modeling, design, & fabrication.

6 Acknowledgements

Orbital trajectory designed by Gabriel Soto in his paper, *“Optimization of high-inclination orbits using planetary flybys for a zodiacal light-imaging mission”*[1]

Zodi CubeSat CAD model designed by Aaron Brown (featured in Figure 1 and Figure 2).

Appendices

A Mass & Volume Budget

Table 14: Mass & Budget for the Zodi CubeSat

Hardware	Mass (kg)	Volume (cm^3)	Volume (U)	Comments & References
BET Thruster	1.15kg/0.329kg	$1000cm^3/333.3cm^3$	1U/0.333U	(BET-1mN/BET-100 μ N)[13][12]
Electrospray Thruster Fuel (Ionic Fluid)	0.037002635kg	$24.18472905cm^3$	0.024184729U	Fuel: 1-Ethyl-3-methylimidazolium bis(trifluoromethylsulfonyl)imide (MW=391.31g/mol, $\rho=1.53g/cm^3$)
RWA (4 Wheels)	0.96kg	$336.4cm^3$	0.3364U	Blue Canyon RWP050[24]
X-Band Transmitter	0.15kg	$92.16cm^3$	0.09216U	CPUT XTX [17]
Omni-Directional X-Band Antenna	0.12kg	$45.61592533cm^3$	0.045615925U	Alaris OMNI-A0150 [18]
Camera	1kg	$1000cm^3$	1U	ADCS-2120 Monochrome Image Sensor [2] with Cassegrain optical system [3]. 1kg mass and 1U volume assumed.
Solar Array	0.06kg	$60cm^3$	0.06U	$1200cm^2$ worth of AzurSpace Solar Cells [20]
Momentum-Dumping System Fuel	0.003741844kg	$2.588475718cm^3$	0.002588476U	See Section 4.6 for derivation
Battery	0.5kg	$333.3333333cm^3$	0.333333333U	0.5kg mass assumed.
Other Electronics & Circuitry	0.5kg	$1000cm^3$	1U	Assumed
Structure	0.745kg	N/A	N/A	ISIS Modular Structure for 4U CubeSat[26]
Total:	5.226kg / 4.399kg	$3894.282cm^3 / 3227.615cm^3$	3.89U / 3.22U	Total with BET-1mN / BET-100 μ N

B Power Budget

Table 15: Power Budget for the Zodi CubeSat

Hardware	Nominal Power Usage (W)	Maximum Power Usage (W)	Comments & References
BET Thruster	5.5/15	5.5/15	(BET-1mN/BET-100 μ N)[13][12]
RWA (4 Wheels)	2	4	Blue Canyon RWP050[24]
Startracker & Sun Sensor	1	1	Assumed
X-Band Transmitter	10	10	CPUT XTX [17]
Omni-Directional X-Band Antenna	5	5	Alaris OMNI-A0150 [18]
Camera	0.15	0.2	ADCS-2120 Monochrome Image Sensor [2]
TMR Microcontroller System	3.6	4	3 Raspberry Pi Model 3B+'s [19]
Data Storage Device	0.5	1	Assumed (Overestimation)
Total while Executing Inclination Change	12.6/22.1	15.5/25	Thruster + RWA + Star/Sun Sensor + Microcontrollers + Data Storage
Total while in Standby/Transit	7.1	10	RWA + Star/Sun Sensor + Microcontrollers + Data Storage
Total while Imaging Zodi Cloud	7.25	10.2	RWA + Star/Sun Sensor + Microcontrollers + Data Storage + Camera
Total while Transmitting	22.1	25	RWA + Star/Sun Sensor + Microcontrollers + Data Storage + Transmitter + Antenna

C Link Budget

Table 16: Link Budget for the Zodi CubeSat

Parameter	NEN Ground Terminal	DSN Ground Terminal	Comments & References
Downlink Frequency	8.45 GHz	8.45 GHz	X-Band
Transmission Dist.	8371 km	8371 km	Given
RF Transmit Power	2W (3.010299957 dBW)	2W (3.010299957 dBW)	From CPUT XTX Datasheet [17]
Antenna Gain	4 dBi	4 dBi	From Alaris OMNI-A0150 Datasheet [18]
Satellite Line Loss (L_{line})	-2 dB	-2 dB	Assumed
Equivalent Isotropic Radiated Power (EIRP)	5.010299957 dBW	5.010299957 dBW	Calculated (See Below)
Free Space Loss (L_s)	-189.442681 dB	-189.442681 dB	Calculated (See Below)
Worst-Case Atmospheric Loss (L_a)	-2.74 dB (Hawaii at 99% Availability)	-0.205 dB (Canberra DSCC at 99% Availability)	NEN User Handbook[27] and DSN User Handbook[28]
Ground Terminal Losses (L_i)	-3 dB	-3 dB	Assumed
Combined External Losses (L_{Comb})	-195.182681 dB	-192.647681 dB	Calculated (See Below)
Worst-Case Receiver G/T	24.4 dB/K (Chile, using largest available antennas)	51.3 dB/K (Worst case G/T for 8.4-8.5 GHz downlink freq. range)	NEN User Handbook[27] and DSN User Handbook[28]
Receiver Carrier-to-Noise Ratio (C/N_0)	62.82761894 dB	92.26261894 dB	Calculated (See Below)
Maximum Allowed Datarate to Obtain 3dB Link Margin	0.392430 Mbps	344.5576478 Mbps	Calculated (See Below)
Chosen Transmission Datarate	0.392430 Mbps	40 Mbps	Chosen
Time to Transmit Collected Image Data (2720Mb)	6931.1724 sec (1.9253 hours)	68 sec	Calculated (See Below)
Required Signal-to-Noise Ratio ($\frac{E_b}{N_0 Req}$)	3.89 dB	3.89 dB	QPSK Modulation with 9/10 Code Rate
Predicted Signal-to-Noise Ratio ($\frac{E_b}{N_0 Pred}$)	6.889996935 dB	16.24201903 dB	Calculated (See Below)
Link Margin	3 dB	12.35201903 dB	Calculated (See Below)

The CubeSat will transmit in the X-Band at 8.45GHz. The X-Band was chosen due to its high datarate capabilities and legacy for deep-space science missions. Based on the CPUT XTX X-Band Transmitter [17] and Alaris OMNI-A0150 High Gain X-Band Omni-directional Antenna [18], a link budget (Table 16 above) was assembled for both the Deep Space Network (DSN) and Near Earth Network (NEN) as potential ground receivers. Based on the CPUT Transmitter datasheet, a RF power of 2W (3dBW) was chosen and the datarate was not allowed to exceed 50Mbps, keeping within the CPUT Transmitter's limits. Similarly, based on the OMNI-A0150 Antenna datasheet, an antenna gain of 4dBi was chosen based on the OMNI-A0150's limits. A satellite line loss, L_{line} , of 2 dB was assumed based on typical satellite line loss values. From these values, the Equivalent Isotropic Radiated Power (EIRP) was calculated:

$$\begin{aligned} EIRP &= P_{Tx}[dBW] + G_{Tx}[dBi] - L_{line}[dB] \\ EIRP &= (3.010299957 \text{ dBW}) + (4 \text{ dBi}) - (2 \text{ dB}) \\ EIRP &= 5.010299957 \text{ dBW} \end{aligned}$$

At this transmission frequency of 8.45GHz and distance of 8731km, free space loss, L_s , amounts to 189.442681dB, as calculated below (where r is distance in km and f is carrier frequency in GHz):

$$\begin{aligned} L_s &= 92.45 + 20 \log(r[km]) + 20 \log(f[GHz]) \\ L_s &= 92.45 + 20 \log(8371 \text{ km}) + 20 \log(8.45 \text{ GHz}) \\ L_s &= 189.442681 \text{ dB} \end{aligned}$$

To ensure our communications system will be able to transmit its data under any atmospheric conditions, worst-case atmospheric losses, L_a , in the X-Band were taken for both the DSN and NEN, resulting in a worst-case atmospheric loss of 0.205dB for the DSN (Canberra DSCC at 99% Availability) and 2.74dB for the NEN (Hawaii at 99% availability). A ground terminal loss, L_i , of 3 dB was assumed based on typical ground terminal loss values. Combining all external losses, L_{Comb} :

$$\begin{aligned} L_{Comb} &= L_s + L_a + L_i \\ L_{CombDSN} &= (189.442681 \text{ dB}) + (0.205 \text{ dB}) + (3 \text{ dB}) = 192.647681 \text{ dB} \\ L_{CombNEN} &= (189.442681 \text{ dB}) + (2.74 \text{ dB}) + (3 \text{ dB}) = 195.182681 \text{ dB} \end{aligned}$$

To ensure our communications system will be able to transmit to ANY ground station in the DSN or NEN, the worst case receiver G/T was taken for both the DSN and NEN, resulting in a worst case G/T of 51.3dB/K for the DSN (worst case for 8.4-8.5 GHz downlink frequency range) and 24.4dB/K for the NEN (Chile, using largest available antenna). Using these worst-case G/T values, the EIRP, and combined external losses (L_{Comb}), the receiver Carrier-to-Noise Ratio, C/N_0 , was calculated:

$$C/N_0 = EIRP + G/T - L_{Comb} + 228.6$$

$$(C/N_0)_{DSN} = (5.010299957 \text{ dBW}) + (51.3 \text{ dB/K}) - (192.647681 \text{ dB}) + 228.6 = 92.26261894 \text{ dB}$$

$$(C/N_0)_{NEN} = (5.010299957 \text{ dBW}) + (24.4 \text{ dB/K}) - (195.182681 \text{ dB}) + 228.6 = 62.82761894 \text{ dB}$$

Our transmitter will use QPSK modulation with a 9/10 code rate, resulting in a required signal-to-noise ratio ($\frac{E_b}{N_0 \text{ Req}}$) of 3.89dB. In order to account for uncertainty, a link margin of at least 3dB was chosen. From this, the maximum allowed datarate, $R_b \text{ Max}$, (in Mbps) in order to achieve a 3dB link margin was calculated:

$$R_b \text{ Max} = \frac{10^{(C/N_0) - (\frac{E_b}{N_0 \text{ Req}}) - (\text{LinkMargin})/10}}{1000000 \text{ bps}}$$

$$R_b \text{ Max DSN} = \frac{10^{(92.26261894 \text{ dB}) - (3.89 \text{ dB}) - (3 \text{ dB})/10}}{1000000 \text{ bps}} = 344.5576478 \text{ Mbps}$$

$$R_b \text{ Max NEN} = \frac{10^{(62.82761894 \text{ dB}) - (3.89 \text{ dB}) - (3 \text{ dB})/10}}{1000000 \text{ bps}} = 0.392430 \text{ Mbps}$$

The transmitter has a maximum datarate of 50 Mbps, so we chose a 40 Mbps datarate when transmitting to the DSN, and a 0.392430 Mbps datarate when transmitting to the NEN. Because two full horizons of images will take up approximately 1360 Mb and the data storage system incorporates a data redundancy of 2, there will be 2720 Mb of data to transmit to Earth. With our selected datarates, it would take $\frac{2720 \text{ Mb}}{40 \text{ Mbps}} = 68 \text{ s}$ to transmit this data to the DSN and $\frac{2720 \text{ Mb}}{0.392430 \text{ Mbps}} = 6931.1724 \text{ s} = 1.9253 \text{ hours}$ to transmit this data to the NEN.

These selected datarates result in the following predicted signal-to-noise ratio ($\frac{E_b}{N_0 \text{ Pred}}$):

$$\frac{E_b}{N_0 \text{ Pred}} = C/N_0 - 10 \log (R_b[\text{bps}])$$

$$\frac{E_b}{N_0 \text{ Pred DSN}} = (92.26261894) - 10 \log (40000000 \text{ bps}) = 16.24201903 \text{ dB}$$

$$\frac{E_b}{N_0 \text{ Pred NEN}} = (62.82761894) - 10 \log (392430 \text{ bps}) = 6.889996935 \text{ dB}$$

Thus resulting in the following link margins:

$$\text{Link Margin} = \frac{E_b}{N_0 \text{ Pred}} - \frac{E_b}{N_0 \text{ Req}}$$

$$\text{Link Margin}_{DSN} = \frac{E_b}{N_0 \text{ Pred DSN}} - \frac{E_b}{N_0 \text{ Req}} = (16.24201903 \text{ dB}) - (3.89 \text{ dB}) = 12.35201903 \text{ dB}$$

$$\text{Link Margin}_{NEN} = \frac{E_b}{N_0 \text{ Pred NEN}} - \frac{E_b}{N_0 \text{ Req}} = (6.889996935 \text{ dB}) - (3.89 \text{ dB}) = 2.999996935 \text{ dB} \approx 3 \text{ dB}$$

D MATLAB Code

D.1 ZODItrajectory.m

```

% Dante Del Terzo (dnd37)
%
% Calculates the distance of our ZODI CubeSat from the sun at a given
  ↪ time
% base on Gabriel Soto's trajectory data. From this distance data,
5 % trajectory, time of simulation, indices of points of interest,
% solar array sizing and power generation, battery sizing,
% external angular momentum, and momentum dumping system sizing are
% calculated.
% Solar array power generation and trajectory are plotted.
10
function ZODItrajectory
load('ZODIstatesAfterFinalFlyby.mat')

%% Trajectory & Orbit Info
15 X = ZODI_afterFirstFlyby(1,:);
Y = ZODI_afterFirstFlyby(2,:);
Z = ZODI_afterFirstFlyby(3,:);

DistMatrix = zeros(1,30000);
20 VelMatrix = zeros(1,30000);
for j = 1:1:30000 %Calculate Distance from Sun at each Point
    D=sqrt(((ZODI_afterFirstFlyby(1,j))^2)+((ZODI_afterFirstFlyby(2,j))^2)+((
        ↪ ZODI_afterFirstFlyby(3,j))^2));
    V=sqrt(((ZODI_afterFirstFlyby(4,j))^2)+((ZODI_afterFirstFlyby(5,j))^2)+((
        ↪ ZODI_afterFirstFlyby(6,j))^2));
    DistMatrix(1,j)=D;
25    VelMatrix(1,j)=V;
end
[Periapsis,PeriIndex] = min(DistMatrix(1,1:15650));
[Apoapsis,ApoIndex] = max(DistMatrix(1,1:15650));
Inclination = asind((ZODI_afterFirstFlyby(3,ApoIndex))/(DistMatrix(ApoIndex)));
30 a = (Apoapsis+Periapsis)/2; %km
eccentricity = (Apoapsis-Periapsis)/(Apoapsis+Periapsis);
b = a*sqrt(1-(eccentricity^2)); %km
SemiP = a*(1-(eccentricity^2)); %km %Semi-Parameter or Semi-Latus Rectum
Period = (1.99622876254e-10)*((a)^(3/2)); %days
35 n = (2*pi)/(Period*24*60*60); %rad/s

% Determine the total simulation time based on the period and the
  ↪ knowledge
% that the simulation ends after intercepting Earth's orbit 3 times
% (determined by inspection)
40 [M, InterceptIndex] = min(abs(ZODI_afterFirstFlyby(1,5:15650)-ZODI_afterFirstFlyby(1,1))+
    ↪ abs(ZODI_afterFirstFlyby(2,5:15650)-ZODI_afterFirstFlyby(2,1)));
FinalTime=((30000)/(3*InterceptIndex))*(3*Period);
%Time_until_Intercept = linspace(0,Period,InterceptIndex);
Time_of_Sim = linspace(0,(FinalTime*24*60*60),30000);
%Time Between Datapoints = 2304.699 sec = 38.4117 min = 0.026675 days
45 %Thus, one day spans approx. 38 datapoints (37.4886 days exactly)

```

```

%[M, InterceptIndex] = min(abs((Time_of_Sim./(60.*60.*24))-Period)); %
    ↪ Find point of Earth Intercept

%Flyby Velocity of Earth During Transmission
EarthFlybyVel = VelMatrix(1,InterceptIndex); %km/s

50 %Time Req To Transmit Data To Earth (From Link Budget)
MaxTransmitTimeSecDSN = (2*34); %sec
MaxTransmitTimeSecNEN = (2*3465.586219); %sec

55 MaxTransmitTimeSec = MaxTransmitTimeSecNEN*2.1; %sec * safety factor of 2.1
MaxTransmitTimeHr = (MaxTransmitTimeSec/(60*60)); %hours

% Will take 9.67 days to capture full horizon at periapsis and apoapsis
% If each timestep is 2304.699 sec, then Periapsis photos will be taken
    ↪ at
60 % indices 2566-2930, Apoapsis photos will be taken at indices 9413-9777.
% Will pass by Earth for transmission at index 13690

PeriSpan = round(round(((9.67*24*60*60)/(Time_of_Sim(1,2)-Time_of_Sim(1,1))),0)/2,0);
ApoSpan = round(round(((9.67*24*60*60)/(Time_of_Sim(1,2)-Time_of_Sim(1,1))),0)/2,0);
65 EarthSpan = round(round(((MaxTransmitTimeHr*60*60)/(Time_of_Sim(1,2)-Time_of_Sim(1,1))),0)
    ↪ /2,0);

TimeBTWDeployAndPeriData = Time_of_Sim(1,PeriIndex-PeriSpan)-Time_of_Sim(1,1);
TimeBTWPeriDataAndApoData = Time_of_Sim(1,ApoIndex-ApoSpan)-Time_of_Sim(1,PeriIndex+PeriSpan
    ↪ );
TimeBTWApoDataAndEarthTransmit = Time_of_Sim(1,InterceptIndex-EarthSpan)-Time_of_Sim(1,
    ↪ ApoIndex+ApoSpan);

70 fprintf(['R_periapsis: ', num2str(Periapsis), ' km\nV_periapsis: ', num2str(VelMatrix(
    ↪ PeriIndex)), ' km/s\nPeriIndex: ', num2str(PeriIndex), '\n\n'])
fprintf(['R_apoapsis: ', num2str(Apoapsis), ' km\nV_apoapsis: ', num2str(VelMatrix(ApoIndex
    ↪ )), ' km/s\nApoIndex: ', num2str(ApoIndex), '\n\n'])
fprintf(['Orbital Elements:\na = ', num2str(a), ' km\np = ', num2str(SemiP), ' km\ne = ',
    ↪ num2str(eccentricity), '\ni = ', num2str(Inclination), ' deg\nn = ', num2str(n), '
    ↪ rad/s\nPeriod = ', num2str(Period), ' days\n\n'])
fprintf(['Total Time of Simulation = ', num2str(FinalTime), ' days\n', 'Time Between Datapoints
    ↪ = ', num2str(Time_of_Sim(1,2)-Time_of_Sim(1,1)), ' sec = ', num2str((Time_of_Sim
    ↪ (1,2)-Time_of_Sim(1,1))/60), ' min\n'])
75 fprintf(['Time Between Orbit Insertion & Peri Data Collect = ', num2str(
    ↪ TimeBTWDeployAndPeriData), ' sec = ', num2str(TimeBTWDeployAndPeriData/(60*60)), '
    ↪ hours = ', num2str(TimeBTWDeployAndPeriData/(60*60*24)), ' days\n'])
fprintf(['Time Between Peri Data & Apo Data Collect = ', num2str(TimeBTWPeriDataAndApoData),
    ↪ ' sec = ', num2str(TimeBTWPeriDataAndApoData/(60*60)), ' hours = ', num2str(
    ↪ TimeBTWPeriDataAndApoData/(60*60*24)), ' days\n'])
fprintf(['Time Between Apo Data Collect & Earth Transmit = ', num2str(
    ↪ TimeBTWApoDataAndEarthTransmit), ' sec = ', num2str(TimeBTWApoDataAndEarthTransmit
    ↪ /(60*60)), ' hours = ', num2str(TimeBTWApoDataAndEarthTransmit/(60*60*24)), ' days\n'
    ↪ ])
fprintf(['Index of Earth Transmit: ', num2str(InterceptIndex), '\n\n'])
fprintf(['Time Req To Transmit Data to Earth (DSN): ', num2str(MaxTransmitTimeSecDSN), ' sec
    ↪ = ', num2str(MaxTransmitTimeSecDSN/(60*60)), ' hours\n'])
80 fprintf(['Time Req To Transmit Data to Earth (NEN): ', num2str(MaxTransmitTimeSecNEN), ' sec
    ↪ = ', num2str(MaxTransmitTimeSecNEN/(60*60)), ' hours\n\n'])

```

```

%% Solar Panel Power Generation
% Calculate and Plot Power Generation based on Distance

85 %Solar Panel Efficiencies
TripleGaAs = 0.28; BOLInherentDegradation = 0.7225; ThetaIncidence = 9.7725;%deg
GaAs = 0.185;
Si = 0.148;

90 % Lifetime Radiation Degredation:

%Based on ZODIpanelDegradation.m, total 1MeV electron fluence that Solar
%Panels will experience per cm^2 in its 700 day lifespan (with no cover
%glass shielding) is 2.383073051704231e+15. This is likely an
    ↪ overestimate.

95 %This maps to a degradation in power of 0.85 according to http://www.
    ↪ spectrolab.com/pv/support/R.%20King%20et%20al.,%20WCPEC%202006,%20
    ↪ Advanced%20III-V%20MJ%20cells%20for%20space.pdf
% for their Ultra-Triple-Junction Cell.
%This maps to a degradation in power of ~0.85 according to http://www.
    ↪ azurspace.com/images/products/0004148-00-01_DB_GBK_80%C2%B5m.pdf
% for their Triple-Junction.
100 %But this is, again, a very rough estimate, so let's assume a
%power degradation of 0.80 by EOL to be extra safe. This is in line with
%solar panel degradation data from the NASA GaAs Radiation Handbook:
%https://ntrs.nasa.gov/archive/nasa/casi.ntrs.nasa.gov/19970010878.pdf
%for a 2 year mission back in 1996.
105 EOLDegrade = 0.80;
%NOTE, this degradation value is most accurate for Triple-Junction GaAs
%cells, but this code applies it to all cell cases

%Constants
110 SolarConst = 1368; %W/m^2
OneAU = 1.496e11; %m

StandbyPower = 10;%W %From Power Budget (Suntracking Software + Pointing
    ↪ Solar Panels Toward Sun)

115 %Calculations
EOLTripleGaAsPowerMatrix = zeros(1,30000);
EOLGaAsPowerMatrix = zeros(1,30000);
EOLSiPowerMatrix = zeros(1,30000);
PDensityMatrix = zeros(1,30000);
120 for p = 1:1:30000 %Calculate Power based on Distance from Sun at each Point
    Dist = DistMatrix(1,p)*1000;%m
    PDensity = (SolarConst)*((OneAU^2)/(Dist^2));
    EOLTripleGaAsPowerMatrix(1,p)=PDensity*TripleGaAs*(BOLInherentDegradation*cosd(
        ↪ ThetaIncidence))*EOLDegrade;
    EOLGaAsPowerMatrix(1,p)=PDensity*GaAs*(BOLInherentDegradation*cosd(ThetaIncidence))*
        ↪ EOLDegrade;
125    EOLSiPowerMatrix(1,p)=PDensity*Si*(BOLInherentDegradation*cosd(ThetaIncidence))*
        ↪ EOLDegrade;
    PDensityMatrix(1,p)=PDensity;
end

```

```

130 % Number of 10x10cm Solar Panels
NumOfPanels = 12; %Number of 10x10cm panels incident on sun

% Therefore, we can calculate power generated in between mission states:
PowerB4PeriTripleGaAs = sum((EOLTripleGaAsPowerMatrix(1,1:(PeriIndex-PeriSpan)).*0.01*
    ↪ NumOfPanels).*(Time_of_Sim(1,2)-Time_of_Sim(1,1)) - StandbyPower.*(Time_of_Sim(1,2)-
    ↪ Time_of_Sim(1,1)));
PowerB4PeriGaAs = sum((EOLGaAsPowerMatrix(1,1:(PeriIndex-PeriSpan)).*0.01*NumOfPanels).*(
    ↪ Time_of_Sim(1,2)-Time_of_Sim(1,1)) - StandbyPower.*(Time_of_Sim(1,2)-Time_of_Sim(1,1)
    ↪ ));
135 PowerB4PeriSi = sum((EOLSiPowerMatrix(1,1:(PeriIndex-PeriSpan)).*0.01*NumOfPanels).*(
    ↪ Time_of_Sim(1,2)-Time_of_Sim(1,1)) - StandbyPower.*(Time_of_Sim(1,2)-Time_of_Sim(1,1)
    ↪ ));

PowerB4ApoTripleGaAs = sum((EOLTripleGaAsPowerMatrix(1,(PeriIndex+PeriSpan):(ApoIndex-
    ↪ ApoSpan)).*0.01*NumOfPanels).*(Time_of_Sim(1,2)-Time_of_Sim(1,1)) - StandbyPower.*(
    ↪ Time_of_Sim(1,2)-Time_of_Sim(1,1)));
PowerB4ApoGaAs = sum((EOLGaAsPowerMatrix(1,(PeriIndex+PeriSpan):(ApoIndex-ApoSpan)).*0.01*
    ↪ NumOfPanels).*(Time_of_Sim(1,2)-Time_of_Sim(1,1)) - StandbyPower.*(Time_of_Sim(1,2)-
    ↪ Time_of_Sim(1,1)));
PowerB4ApoSi = sum((EOLSiPowerMatrix(1,(PeriIndex+PeriSpan):(ApoIndex-ApoSpan)).*0.01*
    ↪ NumOfPanels).*(Time_of_Sim(1,2)-Time_of_Sim(1,1)) - StandbyPower.*(Time_of_Sim(1,2)-
    ↪ Time_of_Sim(1,1)));
140 PowerB4EarthTripleGaAs = sum((EOLTripleGaAsPowerMatrix(1,(ApoIndex+ApoSpan):InterceptIndex)
    ↪ .*0.01*NumOfPanels).*(Time_of_Sim(1,2)-Time_of_Sim(1,1)) - StandbyPower.*(Time_of_Sim
    ↪ (1,2)-Time_of_Sim(1,1)));
PowerB4EarthGaAs = sum((EOLGaAsPowerMatrix(1,(ApoIndex+ApoSpan):InterceptIndex).*0.01*
    ↪ NumOfPanels).*(Time_of_Sim(1,2)-Time_of_Sim(1,1)) - StandbyPower.*(Time_of_Sim(1,2)-
    ↪ Time_of_Sim(1,1)));
PowerB4EarthSi = sum((EOLSiPowerMatrix(1,(ApoIndex+ApoSpan):InterceptIndex).*0.01*
    ↪ NumOfPanels).*(Time_of_Sim(1,2)-Time_of_Sim(1,1)) - StandbyPower.*(Time_of_Sim(1,2)-
    ↪ Time_of_Sim(1,1)));
145 fprintf(['Power Used In Transit (Standby): ' num2str(StandbyPower) ' W\n'])
fprintf(['Number of 10x10cm Solar Panels: ' num2str(NumOfPanels) '\n\n'])
fprintf(['Power Generated In Transit: \n'])
fprintf([' Power Generated Before Periapsis: \n Triple Junc GaAs: ', num2str(
    ↪ PowerB4PeriTripleGaAs),' W*s\n GaAs: ', num2str(PowerB4PeriGaAs),' W*s\n Si: ',
    ↪ num2str(PowerB4PeriSi),' W*s\n\n'])
fprintf([' Power Generated Between Periapsis and Apoapsis: \n Triple Junc GaAs: ', num2str(
    ↪ PowerB4ApoTripleGaAs),' W*s\n GaAs: ', num2str(PowerB4ApoGaAs),' W*s\n Si: ',
    ↪ num2str(PowerB4ApoSi),' W*s\n\n'])
150 fprintf([' Power Generated Between Apoapsis and Earth Transmission: \n Triple Junc GaAs: ',
    ↪ num2str(PowerB4EarthTripleGaAs),' W*s\n GaAs: ', num2str(PowerB4EarthGaAs),' W*s\n
    ↪ Si: ', num2str(PowerB4EarthSi),' W*s\n\n'])

% Plotting Power Generation [MOVED TO END OF CODE]

%% Battery & Solar Panel Sizing
155 % Based on our power budget, the required power at each point of interest
% will be the following (assuming no thruster needed and no transmission
    ↪ unless passing earth):

```

```

% Max Power From Power Budget
PowerReqAtPeri = (5+5+0.2); %W
160 PowerReqAtApo = (5+5+0.2); %W
PowerReqAtEarth = (5+5+10+5); %W

PeriPowerNeed = PowerReqAtPeri*(9.67*24); %W*h
ApoPowerNeed = PowerReqAtApo*(9.67*24); %W*h
165 EarthPowerNeed = PowerReqAtEarth*(MaxTransmitTimeHr); %W*h

% Let us also assume that our power bus will ensure that our batteries
  ↪ are
% fully charged upon reaching a point of interest. In between points of
% interest let us assume that the craft will operate entirely off of
  ↪ solar
170 % power and charge the batteries.

% Self-Discharge Values (from SMAD)
LiIonDischarge = 0.003; % 0.3% per day
NiCdDischarge = 0.01; % 1% per day
175 NiH2Discharge = 0.10; % 10% per day

%Energy Densities in (W*h)/m^3
LiIonEDensity = 250/0.001;%Wh/m^3 %(Ranging from 250–693 Wh/L) From Wikipedia:
  ↪ https://en.wikipedia.org/wiki/Lithium-ion\_battery
NiCdEDensity = 150/0.001;%Wh/m^3 %(Ranging from 50–150 Wh/L) From Wikipedia:
  ↪ https://en.wikipedia.org/wiki/Nickel%E2%80%93cadmium\_battery
180 NiH2EDensity = 60/0.001;%Wh/m^3 %(~60 Wh/L) From Wikipedia: https://en.
  ↪ wikipedia.org/wiki/Nickel%E2%80%93hydrogen\\_battery

% Min 10x10cm Panels Needed for Power Balance

syms TripleGaAsPanels GaAsPanels SiPanels real
185 MinNumOfPanels_TripleGaAs = max([double(solve((ApoPowerNeed)-(sum((
  ↪ EOLTripleGaAsPowerMatrix(1,(ApoIndex-ApoSpan):(ApoIndex+ApoSpan)).*0.01*
  ↪ TripleGaAsPanels).*(Time_of_Sim(1,2)-Time_of_Sim(1,1)))*2.778e-4),TripleGaAsPanels)),
  ↪ double(solve((EarthPowerNeed)-(sum((EOLTripleGaAsPowerMatrix(1,(InterceptIndex-
  ↪ EarthSpan):(InterceptIndex+EarthSpan)).*0.01*TripleGaAsPanels).*(Time_of_Sim(1,2)-
  ↪ Time_of_Sim(1,1)))*2.778e-4),TripleGaAsPanels))]);
MinNumOfPanels_GaAs = max([double(solve((ApoPowerNeed)-(sum((EOLGaAsPowerMatrix(1,(
  ↪ ApoIndex-ApoSpan):(ApoIndex+ApoSpan)).*0.01*GaAsPanels).*(Time_of_Sim(1,2)-
  ↪ Time_of_Sim(1,1)))*2.778e-4),GaAsPanels)),double(solve((EarthPowerNeed)-(sum((
  ↪ EOLGaAsPowerMatrix(1,(InterceptIndex-EarthSpan):(InterceptIndex+EarthSpan)).*0.01*
  ↪ GaAsPanels).*(Time_of_Sim(1,2)-Time_of_Sim(1,1)))*2.778e-4),GaAsPanels))]);
MinNumOfPanels_Si = max([double(solve((ApoPowerNeed)-(sum((EOLSiPowerMatrix(1,(ApoIndex-
  ↪ ApoSpan):(ApoIndex+ApoSpan)).*0.01*SiPanels).*(Time_of_Sim(1,2)-Time_of_Sim(1,1))
  ↪ *2.778e-4),SiPanels)),double(solve((EarthPowerNeed)-(sum((EOLSiPowerMatrix(1,(
  ↪ InterceptIndex-EarthSpan):(InterceptIndex+EarthSpan)).*0.01*SiPanels).*(Time_of_Sim
  ↪ (1,2)-Time_of_Sim(1,1)))*2.778e-4),SiPanels))]);

190 %Power Generated By Solar Panels At Points of Interest in W*h

PowerATPeriTripleGaAs_Wh = sum((EOLTripleGaAsPowerMatrix(1,(PeriIndex-PeriSpan):(PeriIndex+
  ↪ PeriSpan)).*0.01*NumOfPanels).*(Time_of_Sim(1,2)-Time_of_Sim(1,1)))*2.778e-4; %
  ↪ 2.778e-4 is conversion from W*s to W*h

```

```

PowerATPeriGaAs_Wh = sum((EOLGaAsPowerMatrix(1,(PeriIndex-PeriSpan):(PeriIndex+PeriSpan))
    ↪ .*0.01*NumOfPanels).*(Time_of_Sim(1,2)-Time_of_Sim(1,1)))*2.778e-4; %2.778e-4 is
    ↪ conversion from W*s to W*h
PowerATPeriSi_Wh = sum((EOLSiPowerMatrix(1,(PeriIndex-PeriSpan):(PeriIndex+PeriSpan))
    ↪ .*0.01*NumOfPanels).*(Time_of_Sim(1,2)-Time_of_Sim(1,1)))*2.778e-4; %2.778e-4 is
    ↪ conversion from W*s to W*h
195 PowerATApoTripleGaAs_Wh = sum((EOLTripleGaAsPowerMatrix(1,(ApoIndex-ApoSpan):(ApoIndex+
    ↪ ApoSpan)).*0.01*NumOfPanels).*(Time_of_Sim(1,2)-Time_of_Sim(1,1)))*2.778e-4; %2.778
    ↪ e-4 is conversion from W*s to W*h
PowerATApoGaAs_Wh = sum((EOLGaAsPowerMatrix(1,(ApoIndex-ApoSpan):(ApoIndex+ApoSpan)).*0.01*
    ↪ NumOfPanels).*(Time_of_Sim(1,2)-Time_of_Sim(1,1)))*2.778e-4; %2.778e-4 is
    ↪ conversion from W*s to W*h
PowerATApoSi_Wh = sum((EOLSiPowerMatrix(1,(ApoIndex-ApoSpan):(ApoIndex+ApoSpan)).*0.01*
    ↪ NumOfPanels).*(Time_of_Sim(1,2)-Time_of_Sim(1,1)))*2.778e-4; %2.778e-4 is
    ↪ conversion from W*s to W*h

200 % Assuming total transmission time of 2 hours max
PowerATEarthTripleGaAs_Wh = sum((EOLTripleGaAsPowerMatrix(1,(InterceptIndex-EarthSpan):(
    ↪ InterceptIndex+EarthSpan)).*0.01*NumOfPanels).*(Time_of_Sim(1,2)-Time_of_Sim(1,1)))
    ↪ *2.778e-4; %2.778e-4 is conversion from W*s to W*h
PowerATEarthGaAs_Wh = sum((EOLGaAsPowerMatrix(1,(InterceptIndex-EarthSpan):(InterceptIndex+
    ↪ EarthSpan)).*0.01*NumOfPanels).*(Time_of_Sim(1,2)-Time_of_Sim(1,1)))*2.778e-4; %
    ↪ 2.778e-4 is conversion from W*s to W*h
PowerATEarthSi_Wh = sum((EOLSiPowerMatrix(1,(InterceptIndex-EarthSpan):(InterceptIndex+
    ↪ EarthSpan)).*0.01*NumOfPanels).*(Time_of_Sim(1,2)-Time_of_Sim(1,1)))*2.778e-4; %
    ↪ 2.778e-4 is conversion from W*s to W*h

205 %Power that Batteries will need to store (Using TripleGaAs Solar Panels)
LiIonPeriBatNeed_TripleGaAs = (PeriPowerNeed - PowerATPeriTripleGaAs_Wh)/((1-LiIonDischarge)
    ↪ ^(9.47)); %W*h needed taking into account battery discharge
LiIonApoBatNeed_TripleGaAs = (ApoPowerNeed - PowerATApoTripleGaAs_Wh)/((1-LiIonDischarge)
    ↪ ^(4.84)); %W*h
LiIonEarthBatNeed_TripleGaAs = (EarthPowerNeed - PowerATEarthTripleGaAs_Wh)/((1-
    ↪ LiIonDischarge)^(MaxTransmitTimeHr/24)); %W*h
210 LiIonEarthBatNeed_Eclipse = (EarthPowerNeed - 0)/((1-LiIonDischarge)^(MaxTransmitTimeHr/24))
    ↪ ; %W*h

NiCdPeriBatNeed_TripleGaAs = (PeriPowerNeed - PowerATPeriTripleGaAs_Wh)/((1-NiCdDischarge)
    ↪ ^(9.47)); %W*h needed taking into account battery discharge
NiCdApoBatNeed_TripleGaAs = (ApoPowerNeed - PowerATApoTripleGaAs_Wh)/((1-NiCdDischarge)
    ↪ ^(4.84)); %W*h
NiCdEarthBatNeed_TripleGaAs = (EarthPowerNeed - PowerATEarthTripleGaAs_Wh)/((1-NiCdDischarge
    ↪ )^(MaxTransmitTimeHr/24)); %W*h
215 NiCdEarthBatNeed_Eclipse = (EarthPowerNeed - 0)/((1-NiCdDischarge)^(MaxTransmitTimeHr/24));
    ↪ %W*h

NiH2PeriBatNeed_TripleGaAs = (PeriPowerNeed - PowerATPeriTripleGaAs_Wh)/((1-NiH2Discharge)
    ↪ ^(9.47)); %W*h needed taking into account battery discharge
NiH2ApoBatNeed_TripleGaAs = (ApoPowerNeed - PowerATApoTripleGaAs_Wh)/((1-NiH2Discharge)
    ↪ ^(4.84)); %W*h
NiH2EarthBatNeed_TripleGaAs = (EarthPowerNeed - PowerATEarthTripleGaAs_Wh)/((1-NiH2Discharge
    ↪ )^(MaxTransmitTimeHr/24)); %W*h

```

```

220 NiH2EarthBatNeed_Eclipse = (EarthPowerNeed - 0)/((1-NiH2Discharge)^(MaxTransmitTimeHr/24));
    ↪ %W*h

[LiIonMaxBatNeed_TripleGaAs LiIonPOIofMaxBat]= max([LiIonPeriBatNeed_TripleGaAs,
    ↪ LiIonApoBatNeed_TripleGaAs, LiIonEarthBatNeed_TripleGaAs]);
[NiCdMaxBatNeed_TripleGaAs NiCdPOIofMaxBat]= max([NiCdPeriBatNeed_TripleGaAs,
    ↪ NiCdApoBatNeed_TripleGaAs, NiCdEarthBatNeed_TripleGaAs]);
225 [NiH2MaxBatNeed_TripleGaAs NiH2POIofMaxBat]= max([NiH2PeriBatNeed_TripleGaAs,
    ↪ NiH2ApoBatNeed_TripleGaAs, NiH2EarthBatNeed_TripleGaAs]);

%Battery Sizing
LiIonVol_TripleGaAs = LiIonMaxBatNeed_TripleGaAs/LiIonEDensity; %m^3
NiCdVol_TripleGaAs = NiCdMaxBatNeed_TripleGaAs/NiCdEDensity; %m^3
230 NiH2Vol_TripleGaAs = NiH2MaxBatNeed_TripleGaAs/NiH2EDensity; %m^3

LiIonVol_TransmitEclipse = LiIonEarthBatNeed_Eclipse/LiIonEDensity; %m^3
NiCdVol_TransmitEclipse = NiCdEarthBatNeed_Eclipse/NiCdEDensity; %m^3
NiH2Vol_TransmitEclipse = NiH2EarthBatNeed_Eclipse/NiH2EDensity; %m^3
235

fprintf(['Minimum Number of 10x10cm (TripleGaAs) Solar Panels to Make Batteries Unnecessary:
    ↪ ' num2str(NumOfPanels_TripleGaAs) '\nMinimum Number of 10x10cm (GaAs) Solar
    ↪ Panels to Make Batteries Unnecessary: ' num2str(NumOfPanels_GaAs) '\nMinimum
    ↪ Number of 10x10cm (Si) Solar Panels to Make Batteries Unnecessary: ' num2str(
    ↪ NumOfPanels_Si) '\nNumber of 10x10cm Solar Panels: ' num2str(NumOfPanels) '\n\n
    ↪ Minimum LiIon Battery Volume: ' num2str(LiIonVol_TripleGaAs) ' m^3 = ' num2str(
    ↪ LiIonVol_TripleGaAs/(0.1*0.1*0.1)) 'U (assuming TripleGaAs Solar Cells)\n Minimum
    ↪ NiCd Battery Volume: ' num2str(NiCdVol_TripleGaAs) ' m^3 = ' num2str(
    ↪ NiCdVol_TripleGaAs/(0.1*0.1*0.1)) 'U (assuming TripleGaAs Solar Cells)\n Minimum NiH2
    ↪ Battery Volume: ' num2str(NiH2Vol_TripleGaAs) ' m^3 = ' num2str(NiH2Vol_TripleGaAs
    ↪ /(0.1*0.1*0.1)) 'U (assuming TripleGaAs Solar Cells)\n\n'])

% Commented out because trajectory data shows that Earth should not
    ↪ eclipse
240 % spacecraft. Moon might? But chances are low.
%fprintf(['Minimum LiIon Battery Volume for Transmitting During Eclipse:
    ↪ ' num2str(LiIonVol_TransmitEclipse) ' m^3\n Minimum NiCd Battery
    ↪ Volume for Transmitting During Eclipse:: ' num2str(
    ↪ NiCdVol_TransmitEclipse) ' m^3\n Minimum NiH2 Battery Volume for
    ↪ Transmitting During Eclipse: ' num2str(NiH2Vol_TransmitEclipse) ' m
    ↪ ^3\n\n'])

%% Attitude Control System Sizing
% Sweeping Angle & Rate Calculations
245

%Max Angular Rate:
% Angular rate will be highest operationally (not counting perturbation
% correction) when the cubesat needs to fixate on a single point and it
    ↪ is
% traveling fastest. This will occur at periapsis
250

ArcDist_Perri = sqrt(((X(PerriIndex)-X(PerriIndex+1))^2)+((Y(PerriIndex)-Y(PerriIndex+1))^2)+((Z(
    ↪ PerriIndex)-Z(PerriIndex+1))^2));
Perri_Angle_rad=2*atan((ArcDist_Perri/2)/DistMatrix(PerriIndex)) %rad

```

```

MaxAngleRate_radpersec=Peri_Angle_rad/((Time_of_Sim(1,PeriIndex+1)-Time_of_Sim(1,PeriIndex))
↳ ) %rad/s

255 %Total Sweep Angle for Apoapsis and Periapsis:

ArcDist_Peritot = sqrt(((X(PeriIndex-PeriSpan)-X(PeriIndex+PeriSpan))^2)+((Y(PeriIndex-
↳ PeriSpan)-Y(PeriIndex+PeriSpan))^2)+((Z(PeriIndex-PeriSpan)-Z(PeriIndex+PeriSpan))^2)
↳ );
ArcDist_Apo_Tot = sqrt(((X(ApoIndex-ApoSpan)-X(ApoIndex+ApoSpan))^2)+((Y(ApoIndex-ApoSpan)-Y
↳ (ApoIndex+ApoSpan))^2)+((Z(ApoIndex-ApoSpan)-Z(ApoIndex+ApoSpan))^2));

260 Peri_Angle_tot_rad = 2*atan((ArcDist_Peritot/2)/DistMatrix(PeriIndex-PeriSpan)) %rad
Apo_Angle_tot_rad = 2*atan((ArcDist_Apo_Tot/2)/DistMatrix(ApoIndex-ApoSpan)) %rad
Peri_Angle_tot_deg = 2*atand((ArcDist_Peritot/2)/DistMatrix(PeriIndex-PeriSpan)); %deg
Apo_Angle_tot_deg = 2*atand((ArcDist_Apo_Tot/2)/DistMatrix(ApoIndex-ApoSpan)); %deg

265 %Disturbances:
% Solar Radiation Pressure:

% The torque imparted by solar radiation pressure is given by Eq 19-5 of
% SMAD (p. 571). Whether or not a torque actually gets imparted is
270 % dependant on the relative positions of center of mass and center of
↳ solar
% radiation pressure. Let us assume we will be able to configure our
% cubesat such that the distance between the center of mass and center of
% solar radiation pressure is 10cm.

275 %Reflectance based on the absorptivity of the solar panels (a=0.91),
↳ where
%R=1/(10^a) (data obtained from azurspace datasheet: http://www.azurspace
↳ .com/images/products/0004148-00-01_DB_GBK_80%C2%B5m.pdf)

SRP_Matrix = zeros(1,30000);
SRPT_Matrix = zeros(1,30000);
280 SRPM_Matrix = zeros(1,30000);
for p = 1:1:30000 %Calculate Solar Radiation Pressure based on Distance from
↳ Sun at each Point
    PDensity = PDensityMatrix(1,p);
    F_SRP = (PDensity/(3e8))*(NumOfPanels*(0.1*0.1))*(1+0.1230)*(Time_of_Sim(1,2)-
↳ Time_of_Sim(1,1)); %N*s
    T_SRP = (PDensity/(3e8))*(NumOfPanels*(0.1*0.1))*(1+0.1230)*(0.1)*cosd(ThetaIncidence);
↳ %Nm % Assuming case of 10cm (0.1m) distance between the center of
↳ mass and center of solar radiation pressure)
285 M_SRP = (PDensity/(3e8))*(NumOfPanels*(0.1*0.1))*(1+0.1230)*(0.1)*cosd(ThetaIncidence)*
↳ (Time_of_Sim(1,2)-Time_of_Sim(1,1)); %Nms %Angular Incidence
    SRP_Matrix(1,p)=F_SRP;
    SRPT_Matrix(1,p)=T_SRP;
    SRPM_Matrix(1,p)=M_SRP;
end

290 Max_SRPImpulse_Ns = max(SRP_Matrix) %N*s
Min_SRPImpulse_Ns = min(SRP_Matrix) %N*s
Total_SRPImpulse_Ns = sum(SRP_Matrix) %N*s

295 Max_SRPTorque_Nm = max(SRPT_Matrix) %N*m

```

```

Min_SRPTorque_Nm = min(SRPT_Matrix) %N*m
%Total_SRPmomentumChange_Nms = sum(SRPM_Matrix(1:13738)) %N*m*s %
    ↪ Propagate only to time index 13738, 24 hours after first earth
    ↪ transmission of 13690
Total_SRPmomentumChangeDuringPhotos_Nms = sum(SRPM_Matrix(1,(ApoIndex-ApoSpan):(ApoIndex+
    ↪ ApoSpan))) + sum(SRPM_Matrix(1,(PeriIndex-PeriSpan):(PeriIndex+PeriSpan))) %Nms &
    ↪ If we assume that the spacecraft will rotate in transit such that it
    ↪ does not build up momentum in transit, then during pointing is the
    ↪ only time when it would build momentum

300 MomentumStorage=0.050; %Nms %Based on http://bluecanyontech.com/rwp050/
Num_Of_Momentum_Dumps = ((Total_SRPmomentumChangeDuringPhotos_Nms)/(4*(MomentumStorage)))
    ↪ *1.2 %1.2 safety factor included

Thruster_MomentArm = 0.1; %m %Assuming largest moment arm distance (distance
    ↪ from thruster to center of mass) is 10cm
Dumping_Burn_Time = 1; %s
305 Momentum_Dumping_Sizing_Force = (Total_SRPmomentumChangeDuringPhotos_Nms)/((
    ↪ Thruster_MomentArm)*(Dumping_Burn_Time)) %N %From Table 19-12 on p. 583 of
    ↪ SMAD

Dumping_Fuel_Isp= 40;
Mass_Of_Dumping_Fuel= (Momentum_Dumping_Sizing_Force*(1.5))*(Num_Of_Momentum_Dumps*
    ↪ Dumping_Burn_Time)/(9.80665*Dumping_Fuel_Isp)
%Using Equation from p. 581 of SMAD, Table 19-11, row 3.
310 %Momentum_Sizing=Max_SRPTorque_Nm*(Time_of_Sim(13800))*(0.707/4)

% Angular Impulse (Total torque over time) is equivalent to change in
% momentum.

315 DoNotPlot this %Uncomment to prevent plotting each time code is run

%% Plots trajectory graph and sets up a custom data tip update function
fig = figure('DeleteFcn','doc datacursormode');

320 plot3(X,Y,Z)
hold on
plot3(0,0,0,'X')
hold off
title(['ZODI Orbital Trajectory After First Flyby (Heliocentric J200)'])
325 grid on
xlabel(['X (km)'])
ylabel(['Y (km)'])
zlabel(['Z (km)'])

330 dcm_obj = datacursormode(fig);
set(dcm_obj, 'UpdateFcn',{@myupdatefcn,ZODI_afterFirstFlyby})

figTOP = figure('DeleteFcn','doc datacursormode');

335 plot(X,Y)
hold on
plot(0,0,'X')
hold off
title(['ZODI Orbital Trajectory After First Flyby (Heliocentric J200) Top-Down'])

```

```

340 grid on
xlabel(['X (km)'])
ylabel(['Y (km)'])

dcm_objTOP = datacursormode(figTOP);
345 set(dcm_objTOP, 'UpdateFcn',{@myupdatefcnTOP,ZODI_afterFirstFlyby})

%% Plotting Power Generation
figPOWER = figure('DeleteFcn','doc datacursormode');

350 plot(Time_of_Sim./(60.*60.*24),EOLTripleGaAsPowerMatrix,Time_of_Sim./(60.*60.*24),
    ↪ EOLGaAsPowerMatrix,Time_of_Sim./(60.*60.*24),EOLSiPowerMatrix,[Time_of_Sim(1,
    ↪ InterceptIndex)./(60.*60.*24) Time_of_Sim(1,InterceptIndex)./(60.*60.*24)], [0 450])
hold on
line([Time_of_Sim(1,15650)./(60.*60.*24) Time_of_Sim(1,15650)
    ↪ ./(60.*60.*24)], [0 450], 'Color', 'red', 'LineStyle', '--')
hold off
title(['EOL Power Generation By Solar Panels over Time'])
355 grid on
xlabel(['Time (days)'])
ylabel(['Power Generation (W/m^2)'])
legend('Triple Junc GaAs','GaAs','Si','Closest to Earth')

360 dcm_objPOWER = datacursormode(figPOWER);
set(dcm_objPOWER, 'UpdateFcn',{@myupdatefcnPOWER,ZODI_afterFirstFlyby})

%% Customize cursor data for each above plot
function txt = myupdatefcn(~,event_obj,ZODI_afterFirstFlyby)
365 % Customizes text of data tips
pos = get(event_obj, 'Position');
I = get(event_obj, 'DataIndex');
txt = {['X: ', num2str(pos(1))], ...
    ['Y: ', num2str(pos(2))], ...
370 ['Z: ', num2str(pos(3))], ...
    ['I: ', num2str(I)], ...
    ['Vx: ', num2str(ZODI_afterFirstFlyby(4,I)), ' km/s'], ...
    ['Vy: ', num2str(ZODI_afterFirstFlyby(5,I)), ' km/s'], ...
    ['Vz: ', num2str(ZODI_afterFirstFlyby(6,I)), ' km/s'], ...
375 ['Dist. Sun: ', num2str(sqrt((pos(1)^2)+(pos(2)^2)+(pos(3)^2)))]];
function txtTOP = myupdatefcnTOP(~,event_obj,ZODI_afterFirstFlyby)
% Customizes text of data tips
pos = get(event_obj, 'Position');
I = get(event_obj, 'DataIndex');
380 txtTOP = {['X: ', num2str(pos(1))], ...
    ['Y: ', num2str(pos(2))], ...
    ['Z: ', num2str(ZODI_afterFirstFlyby(3,I))], ...
    ['I: ', num2str(I)], ...
    ['Vx: ', num2str(ZODI_afterFirstFlyby(4,I)), ' km/s'], ...
385 ['Vy: ', num2str(ZODI_afterFirstFlyby(5,I)), ' km/s'], ...
    ['Vz: ', num2str(ZODI_afterFirstFlyby(6,I)), ' km/s'], ...
    ['Dist. Sun: ', num2str(sqrt((pos(1)^2)+(pos(2)^2)+((ZODI_afterFirstFlyby(3,I))^2)))
    ↪ ]];
function txtPOWER = myupdatefcnPOWER(~,event_obj,ZODI_afterFirstFlyby)
% Customizes text of data tips
390 pos = get(event_obj, 'Position');

```

```

I = get(event_obj, 'DataIndex');
txtPOWER = [['Time: ', num2str(pos(1)), ' days'], ...
            ['Power Generation: ', num2str(pos(2)), ' W/m^2'], ...
            ['I: ', num2str(I)], ...
            ['Dist. Sun: ', num2str(sqrt(((ZODI_afterFirstFlyby(1,I))^2)+((ZODI_afterFirstFlyby(2,
            ↪ I))^2)+((ZODI_afterFirstFlyby(3,I))^2))), ' km']];

```

D.2 ZODIpanelDegradation.m

```

function TotalSolar1MeVFluence=ZODIpanelDegradation
% Dante Del Terzo (dnd37)
%
% Estimates the total electron fluence that the ZODI solar panels will be
5 % subjected to both over the course of its lifetime and when closest to
    ↪ the
% sun in order to size solar panel degradation due to radiation. These
% estimates are very rough and are likely an overestimation of actual
    ↪ solar
% particle fluences. Nevertheless, because of the inexact nature of this
% overestimation, solar panels will be sized assuming a solar fluence
    ↪ even
10 % higher than this code estimates. See the Solar Panel Sizing section of
% "ZODItrajectory.m" for more details.

%% Distance Data
load('ZODIstatesAfterFinalFlyby.mat')
15
X = ZODI_afterFirstFlyby(1,:);
Y = ZODI_afterFirstFlyby(2,:);
Z = ZODI_afterFirstFlyby(3,:);

20 DistMatrix = zeros(1,30000);
VelMatrix = zeros(1,30000);
for j = 1:1:30000 %Calculate Distance from Sun at each Point
    D=sqrt(((ZODI_afterFirstFlyby(1,j))^2)+((ZODI_afterFirstFlyby(2,j))^2)+((
    ↪ ZODI_afterFirstFlyby(3,j))^2));
    V=sqrt(((ZODI_afterFirstFlyby(4,j))^2)+((ZODI_afterFirstFlyby(5,j))^2)+((
    ↪ ZODI_afterFirstFlyby(6,j))^2));
25    DistMatrix(1,j)=D;
    VelMatrix(1,j)=V;
end

Period = 365.1653; %days
30
[M, InterceptIndex] = min(abs(ZODI_afterFirstFlyby(1,5:15650)-ZODI_afterFirstFlyby(1,1))+
    ↪ abs(ZODI_afterFirstFlyby(2,5:15650)-ZODI_afterFirstFlyby(2,1)));
FinalTime=((30000)/(3*InterceptIndex))*(3*Period);
Time_of_Sim = linspace(0,(FinalTime*24*60*60),30000);
%Time Between Datapoints = 2304.699 sec = 38.4117 min = 0.026675 days
35
%% Degradation Calculations & Data

% Using values from Table 1 of https://www.spennis.oma.be/help/background
    ↪ /flare/flare.html

```

```

% which lists the proton fluences (in cm^-2) from solar activity for
  ↪ solar cycles
40 % 20-22 obtained from IMP-3, -4, -5, -7 and -8 satellites (for cycle
  ↪ 20),
% IMP-8 (for cycle 21), and GOES-5, -6 and -7 satellite data (for cycle
% 22).

%Column 1 is proton energy range (in MeV) with energy >E, column 2 is the
45 %minimum event fluence, column 3 is the worst case event fluence. For all
%applications, I will be using the worst case event fluence.
%These values will be further scaled according to an inverse square (1/R
  ↪ ^2)
%dependence on distance from the sun, as all table values were taken from
  ↪ a
%distance of 1AU.

50 SolarEvent = [ 1, 5.0e8, 1.55e11; ...
                3, 1.0e8, 8.71e10; ...
                5, 1.0e8, 6.46e10; ...
                7, 2.5e7, 4.79e10; ...
55                10, 2.5e7, 3.47e10; ...
                15, 1.0e7, 2.45e10; ...
                20, 1.0e7, 1.95e10; ...
                25, 3.0e6, 1.55e10; ...
                30, 3.0e6, 1.32e10; ...
60                35, 3.0e6, 1.17e10; ...
                40, 1.0e6, 8.91e9; ...
                45, 1.0e6, 7.94e9; ...
                50, 3.0e5, 6.03e9; ...
                55, 3.0e5, 5.01e9; ...
65                60, 3.0e5, 4.37e9; ...
                70, 1.0e5, 3.09e9; ...
                80, 1.0e5, 2.29e9; ...
                90, 1.0e5, 1.74e9; ...
                100,1.0e5, 1.41e9];

70 % Damage coefficients pulled from https://ntrs.nasa.gov/archive/nasa/casi
  ↪ .ntrs.nasa.gov/19970010878.pdf
% Table 5.3 (pg.120 of pdf). Only damage coefficients corresponding to
  ↪ energies
% listed in SolarEvent are included. In cases where exact mappings
  ↪ between
% energy and coefficient could not be found, averages were taken.
75 % Column 1 lists damage coefficients with no cover glass (shielding)
% thickness. Column 2 lists damage coefficients with 1mm cover glass
% thickness. Column 3 lists damage coefficients with 3mm cover glass. For
% the following calculations, the no cover glass case (Column 1) damage
% coefficients were used.
80 DamCoefficient = [ 7.40, 0, 0; ... %1MeV
                  3.00, 1.705, 1.544; ... %3MeV
                  1.865, 1.02115, 1.1265; ... %5MeV
                  1.325, 0.7064, 0.78595; ... %7MeV
                  1, 0.5278, 0.5587; ... %10MeV
85                  0.820, 0.403, 0.4091; ... %15MeV
                  0.740, 0.366, 0.3733; ... %20MeV

```

```

    0.695, 0.3424, 0.3433; ... %25MeV
    0.670, 0.3306, 0.3347; ... %30MeV
    0.6475,0.319275,0.319725; ... %35MeV
90    0.635, 0.31285, 0.31305; ... %40MeV
    0.6225,0.30665, 0.30735; ... %45MeV
    0.610, 0.3005, 0.3011; ... %50MeV
    0.600, 0.2955, 0.2959; ... %55MeV
    0.595, 0.2929, 0.2931; ... %60MeV
95    0.580, 0.2856, 0.2860; ... %70MeV
    0.575, 0.2830, 0.2831; ... %80MeV
    0.562, 0.2767, 0.2769; ... %90MeV
    0.560, 0.2756, 0.2756]; %100MeV
SolarFluence=zeros(1,18);
100 for ind = 1:1:18
    SolarFluence(1,ind)=(SolarEvent(ind,3)-SolarEvent(ind+1,3))*DamCoefficient(ind,1);
end
%Cumulative proton fluence per cm^2 per day divided by 1 day in seconds
%multiplied by 1000 factor as described in Table 9.1 of NASA
    ↪ documentation
105 %to convert from the calculated 10MeV proton fluence to 1MeV electron
    ↪ fluence
%equivalent:
%Because the fluence data only pertains to individual solar events, lets
%make the assumption that our SC will experience 3 worst case
%solar events at every energy range within its lifespan. This
110 %assumption is based off of Table 8.3 of the NASA documentation detailing
%actual solar events as well as the fact that the higher fluence events
%cause the most degradation and typically happen more infrequently (thus
    ↪ 3
%high fluence events per lifespan is a believable value and their
    ↪ fluence
%numbers would dominate the others)
115 SolarFluence1MeV=((3*sum(SolarFluence))/(700*24*60*60))*1000; %1MeV electrons per cm
    ↪ ^2 per second at 1AU

OneAU = 1.496e11;
eFluence = zeros(1,30000);
for dd = 1:1:30000 %Calculate Degredation based on Distance from Sun at each
    ↪ Point
120    Dist = DistMatrix(1,dd)*1000;%m
    eFluence(1,dd) = (SolarFluence1MeV)*((OneAU^2)/(Dist^2));
end
TotalSolar1MeVFluence=sum(eFluence.*(Time_of_Sim(1,2)-Time_of_Sim(1,1))); %particles
    ↪ per cm^2 %Over Lifetime
125 %What if 1 worstcase event at every energy level occurs when SC is
    ↪ closest
%to sun? Typical solar ejection events only last a few minutes to hours
WorstCaseCloseToSun_perMin=(SolarFluence1MeV/3).*((OneAU^2)./(108748530.4715^2))*60 %
    ↪ particles per cm^2 per min

```

D.3 ZODIphototime.m

```

function Time = ZODIphototime()
% Dante Del Terzo (dnd37)
%
% Calculates the total integration time (time to take one photo) for the
% Agilent ADCS-2120 monochrome image sensor imaging the Zodiacal Dust
5   ↪ Cloud
% assuming a read time of 1000s and 10cm aperture.

readtime = 1000; %s

10  syms t
    assume(t,'real');
    assume(t>=0);

D = 0.010; %m (10 cm)
15  F0 = 9.5e16; %9500; %(9500e13 photons m(-3) s(-1)) ; (9500 photons cm
    ↪ (-2) nm(-1) s(-1))
QE = 0.38; %percent at peak at 555nm %
A = (pi/4)*(D^2);

DC = 240/(640*480); %(240 electrons/s per pixel area)/(total pixels)

20  %Assumed:
SNratio = 5;
magzodi = 22.5;
lightwavelength = 555e-9; %cm 5.55e-7m (555 nm)
25  band = 88e-9; %nm 8.8e-8 m (88 nm)
T = 0.5;
RN = 1/readtime; %(4 electrons per read)/total read time
%omega = ((lightwavelength./(2.*D)).^2);
omega = (180/pi*3600)^2*((lightwavelength./(2*D)).^2);

30  %Calculation of Signal & Noise
Cs = F0*(10^(-magzodi/2.5))*omega*A*QE*T*band;
%Cs = F0*(10^(-magzodi/2.5))*((pi^2)/4)*(lightwavelength^2)*(0.7^2)*T*
    ↪ band;
Cn = RN + DC;
35  Time = double(solve(SNratio==(Cs*t)/sqrt((Cn*t)),t));

fprintf(['Time to take One Image = ', num2str(Time),' sec = ', num2str(Time/60),' min = ',
    ↪ num2str(Time/(60*60)),' hours\n'])

```

References

- [1] Gabriel Soto, James Lloyd, Dmitry Savransky, Keith Grogan, Amlan Sinha. *Optimization of high-inclination orbits using planetary flybys for a zodiacal light-imaging mission*. Cornell University, SIOS Lab, 2017.
- [2] *Agilent ADCS-1120/ADCS-2120 CMOS Monochrome Image Sensors Datasheet*. Agilent Technologies. 2002. Accessed May 23, 2018. Retrieved from <http://static6.arrow.com/aropdfconversion/a9f85082bcf408de4a648fdc9eba19def1329b70/5988-4650en.pdf>
- [3] Simms, L. M., Riot, V., Vries, W. D., Olivier, S. S., Pertica, A., Bauman, B. J., . . . Nikolaev, S. (2011). **Optical payload for the STARE pathfinder mission**. *Sensors and Systems for Space Applications IV*. doi:10.1117/12.882791. Accessed May 23, 2018. Retrieved from <https://e-reports-ext.llnl.gov/pdf/473852.pdf>
- [4] G. James Wells, Luke Stras, Tiger Jeans. *Canada's Smallest Satellite: The Canadian Advanced Nanospace eXperiment (CanX-1)*. University of Toronto Institute For Aerospace Studies, Space Flight Laboratory, 2003. Accessed May 23, 2018. Retrieved from <http://citeseerx.ist.psu.edu/viewdoc/download?doi=10.1.1.557.7343&rep=rep1&type=pdf>
- [5] Stark, C. C., Roberge, A., Mandell, A., & Robinson, T. D. (2014). **MAXIMIZING THE ExoEarth CANDIDATE YIELD FROM A FUTURE DIRECT IMAGING MISSION**. *The Astrophysical Journal*, 795(2), 122. doi:10.1088/0004-637x/795/2/122. Accessed May 23, 2018. Retrieved from <http://iopscience.iop.org/article/10.1088/0004-637X/795/2/122/meta>
- [6] *UI-1462LE Image Sensor Datasheet*. IDS Imaging Development Systems. 2018. Accessed May 23, 2018. Retrieved from <https://en.ids-imaging.com/store/ui-1462le.html>
- [7] *uCAM-III Image Sensor Datasheet*. Rev 1.0. 4D Systems. 2016. Accessed May 23, 2018. Retrieved from http://www.mouser.com/ds/2/451/uCAM-III_datasheet_R_1_0-1100457.pdf
- [8] *MT9M001C12STM (Monochrome) Datasheet*. Rev M. Semiconductor Components Industries. 2015. Accessed May 23, 2018. Retrieved from <https://www.onsemi.com/pub/Collateral/MT9M001-D.PDF>
- [9] *OV7648 Image Sensor Datasheet*. Omnivision Technologies. n.d.. Accessed May 23, 2018. Retrieved from <http://forum.motofan.ru/index.php?act=Attach&type=post&id=6690>
- [10] *AM41V4 Image Sensor Datasheet*. Rev 1.0. Alexima Technology. 2012. Accessed May 23, 2018. Retrieved from http://www.alexima.com/pub/AM41V4_datasheet.pdf
- [11] *OV7620 Image Sensor Datasheet*. Ver 2.1. Omnivision Technologies. 2001. Accessed May 23, 2018. Retrieved from https://quasarelectronics.co.uk/kit-files/omnivision/ov7620_ov7120_v1.2whole.pdf

- [12] *BET-100 μ N Busek Electrospray Thruster Datasheet*. 70008516. Rev E. Busek Space Propulsion and Systems. 2016. Accessed May 23, 2018. Retrieved from http://www.busek.com/index_htm_files/70008516%20BET-100uN%20Data%20Sheet%20RevE.pdf
- [13] *BET-1mN Busek Electrospray Thruster Datasheet*. 70008500. Rev H. Busek Space Propulsion and Systems. 2016. Accessed May 23, 2018. Retrieved from http://www.busek.com/index_htm_files/70008500%20BET-1mN%20Data%20Sheet%20RevH.pdf
- [14] *Propellantless Field Emission Cathode Datasheet*. 70008503. Rev G. Busek Space Propulsion and Systems. 2016. Accessed May 23, 2018. Retrieved from http://www.busek.com/index_htm_files/70008503G.pdf
- [15] *LISA Pathfinder Press Release*. 70000704. Busek Space Propulsion and Systems. December 03, 2015 & February 01, 2016. Accessed May 23, 2018. Retrieved from http://busek.com/index_htm_files/70000704%20LISA%20Pathfinder%20Release%20Rev-.pdf
- [16] *FIRST FLIGHT ELECTROSPRAY THRUSTER, LISA PATHFINDER (DELIVERED, 2008)*. Busek Space Propulsion and Systems. n.d. Accessed May 23, 2018. Retrieved from http://busek.com/flightprograms__st7.htm
- [17] *CubeSat X-Band Transmitter (XTX) Datasheet*. BR-01-00079. Rev A. Cape Peninsula University of Technology. 2017. Accessed May 23, 2018. Retrieved from <http://www.cput.ac.za/blogs/fsati/files/2016/10/BR-01-00079-XTX-Brochure-Rev-A-Website.pdf>
- [18] *High Gain X-Band Omni Antenna Datasheet*. OMNI-A0150. Rev 1.4. Alaris Antennas. May 21, 2015. Accessed May 23, 2018. Retrieved from <http://www.alarisantennas.com/wp-content/uploads/2017/06/brochures/OMNI-A0150%20Version%201.4.pdf>
- [19] *Raspberry Pi Model 3B+ Datasheet*. Raspberry Pi Foundation. n.d. Accessed May 23, 2018. Retrieved from <https://static.raspberrypi.org/files/product-briefs/Raspberry-Pi-Model-Bplus-Product-Brief.pdf>
- [20] *AzurSpace 30% Triple Junction GaAs Solar Cell Datasheet*. 0004148-00-01. AZUR SPACE. August 19, 2016. Accessed May 23, 2018. Retrieved from http://www.azurspace.com/images/products/0004148-00-01_DB_GBK_80%C2%B5m.pdf
- [21] B. E. Anspaugh. *GaAs Solar Cell Radiation Handbook*. NASA JPL. July 1, 1996. Accessed May 23, 2018. Retrieved from <https://ntrs.nasa.gov/archive/nasa/casi.ntrs.nasa.gov/19970010878.pdf>
- [22] Richard R. King et. al. **ADVANCED III-V MULTIJUNCTION CELLS FOR SPACE**. Spectrolab. *Presented at the 4th World Conference on Photovoltaic Energy Conversion, Waikoloa, Hawaii*. May 7-12, 2006. Accessed May 23, 2018. Retrieved from <http://www.spectrolab.com/pv/support/R.%20King%20et%20al.,%20WCPEC%202006,%20Advanced%20III-V%20MJ%20cells%20for%20space.pdf>

- [23] Mukund R. Patel. *Spacecraft Power Systems*. CRC Press, 2004.
- [24] *Blue Canyon Reaction Wheels Datasheet*. RWP050. Blue Canyon Technologies. n.d.. Accessed May 23, 2018. Retrieved from http://bluecanyontech.com/wp-content/uploads/2018/01/DataSheet_RW_07_F.pdf
- [25] Barucci, M., Risegari, L., Olivieri, E., Pasca, E., & Ventura, G. (2004). Aluminium Alloys For Space Applications: Low Temperature Thermal Conductivity Of A6061-T6 And A1050. *Astroparticle, Particle and Space Physics, Detectors and Medical Physics Applications*. doi:10.1142/9789812702708_0079
- [26] *ISIS CubeSat Structure Brochure*. ISIS: Innovative Solutions in Space. n.d.. Accessed May 23, 2018. Retrieved from https://www.cubesatshop.com/wp-content/uploads/2016/06/ISIS_CubeSat-Structures_Brochure_v.7.11.pdf
- [27] *Near Earth Network (NEN) User Handbook*. NASA. Feb 24, 2016. Accessed May 23, 2018. Retrieved from <https://sbir.gsfc.nasa.gov/sites/default/files/453-NENUG%20R2.pdf>
- [28] *Deep Space Network (DSN) User Handbook*. NASA. Accessed May 23, 2018. Retrieved from <https://deepspace.jpl.nasa.gov/dsndocs/810-005/>
- [29] Wertz, J. R., Everett, D. F., & Puschell, J. J. (2015). *Space Mission Engineering: The New SMAD*. Hawthorne: Microcosm Press.